Addis Ababa University

Addis Ababa Institute of Technology

School of Civil and Environmental Engineering

Hydraulic Engineering Stream

Dam Breach Analysis and Flood Inundation Mapping For Lower Awash Multipurpose Dam

A Thesis Submitted to the School of Graduate Studies of Addis Ababa University in Partial Fulfillment of the Degree of Master of Science in Civil Engineering (Major in Hydraulic Engineering)

By

Addisalem Eyob

Advisor: Daneal F/Selassie (PhD)

November, 2020

Addis Ababa, Ethiopia

The undersigned have examined the thesis entitled **'Dam breach Analysis and Flood Inundation Mapping for Lower Awash Multipurpose Dam'** presented by **Addisalem Eyob**, a candidate for the degree of **Master of Science** and hereby certify that it is worthy of acceptance.

Dr. Daneal F/Selassie	Daneal F/S	17/10/2020
Advisor	Signature	Date
Dr.Ing. Assie Kemal		17/10/2020
Internal Examiner	Signature	Date
Dr. Yilma Seleshi		31/10/2020
External Examiner	Signature	Date
Dr.Ing. Mebruk Mohammed	Mebruk Mohammed (Dr.-Ing.) Dean,School of Civil & Environmental Engineering	
Chair person	Signature	Date

UNDERTAKING

I certify that the thesis work titled “Dam breach Analysis and Flood Inundation Mapping for Lower Awash Multipurpose Dam” is my own work. The work has not been presented somewhere else for evaluation. The material has been used from other sources it has been properly acknowledged.

Addisalem Eyob
aduhydro@gmail.com

November, 2020
Addis Ababa, Ethiopia

ABSTRACT

Dam breach analysis is essential for investigating future effects posed to human life and property by a sudden release of water to the inundation area downstream of a dam. Every constructed as well as proposed dams need to be analyzed for the possibility of dam breach to clearly identify the extent of catastrophic effects associated with their failure. The aim of this study is to model the dam breach at the proposed Lower Awash Dam for the development of flood inundation maps used to emergency action plans.

The proposed dam is located in Afar National Regional State on Logia River at about one hundred kilometers upstream from the bridge on Logia River of main road to Djibouti. The analysis was performed for piping failure scenario using HEC-RAS two dimensional unsteady flow modeling. The inflow hydrograph was taken as an upstream boundary condition for the unsteady flow simulation. The model was calibrated for the flow years (1998-1999) and its performance was evaluated for the year 2001. The flood inundation and flood hazard maps were prepared by exporting the tiff raster files from RAS Mapper to ArcGIS and overlying to ArcGoogle to visualize coverage of the flood prone area due to the breach.

The resulting breach parameters were 146 meters breach bottom width, 1.17 hours breach formation time, and 0.5 breach side slope (H:V). The simulated results on HEC-RAS reached peak breach outflow discharge of 60,072 cumecs. Through model calibration close agreement has been arrived between model simulated and observed rating curves at Logia gauging station. As noticed from the flood inundation and flood hazard maps an extended area in the flat plains downstream of the dam would be affected due to the breach with a maximum flood depth of 21.6 m. Therefore, the flood inundation and flood hazard maps could be adopted for proper emergency action plans that have to be taken by stake holders.

Key words: Lower Awash, HEC-RAS, ArcGIS, RAS Mapper, Dam Breach, Inundation Map

ACKNOWLEDGMENTS

I am greatly indebted to my advisor Dr. Daneal F/Selassie for his support and encouragement during all the course of my study. His critical comments and valuable advices helped me to take this research in the right places. Without him, this study wouldn't have been realized and finalized.

Afterwards, I extend my heartfelt thanks to Mr. Haile Belay for sparing his valuable time whenever I approached him and showing me the way ahead.

I take pride in acknowledging the Ethiopian Construction Design and Supervision Works Corporation, Hydropower & Head Work Staffs for providing me the necessary data, information and guidance to fulfill this thesis work.

I have no words to pay thanks to my mother and all family members for their continuous prayers and moral support. I also like to states my profound gratitude's and appreciation to all my friends and my class mates for their idea sharing.

TABLE OF CONTENTS

LIST OF TABLES

LIST OF FIGURES

ABREVIATIONS

DAMBK	Dam Break-Forecasting Model
DEM	Digital Elevation Model
DSIG	Dam Safety Interests Group
FEMA	Federal Emergency Management Agency
FERC	Federal Energy Regulation Commission
FLDVWAV	Flood wave dynamic modeling
FRL	Full Reservoir Level
GIS	Geographic Information System
GPS	Global Positioning System
HEC	Hydrologic Engineering Centre
HEC-HMS	Hydrologic Engineering Center's Hydrologic Modeling System
HEC-RAS	Hydraulic Engineering Center for River Analysis System
HSG	Hydrologic Soil Group
ICOLD	International Commission on Large Dams
MOWIE	Minister of Water, Irrigation and Energy
NMA	National Meteorological Agency
NRCS	Natural Resource Conservation Services
NWS	National Weather Service
PMF	Probable Maximum Flood
RAS	River Analysis System
SMPDK	Simple Dam Break Model
USACE	United States Army Corps of Engineers
USBR	United States Bureau of Reclamation
UTM	Universal Transverse Mercator
WWDSE	Water Works Design and Supervision Enterprise
2D	Two dimensional

CHAPTER ONE

1. INTRODUCTION

1.1 Background

Construction of dams is highly essential in developing countries. Nowadays there are over half million dams and many kilometers of canals, built in the world to achieve the purposes: such as flood prevention, irrigation development, hydroelectricity generation, drinking water supply, recreation, or any other. (Zagonjolli, M., Dam breaks Modeling, Risk Assessments and Uncertainty Analysis for Flood Mitigation, 2007). At this time an acceptable number of dams are being implemented in Ethiopia, ranging from minor micro earth dams built for community demand to mega schemes such as the Great Ethiopian Renaissance Dam, being implemented to enhance the nation's economy (Tariku Tadesse, 2015).

While planning and implementing dams, giving a good attention for their well performing capacity is come to be a significant matter since lots of dams have been breached out in past in different sides of our world and have leads to a disastrous damage to lives of people, property and the environment in as a whole. The Banqiao Dam and the Shimantan Dam failed catastrophically caused by the overtopping due to heavy rains can be taken as the world's worst dam disaster occurred in Henan province in China, in August 1975,. Roughly about 85,000 people died after flooding and many more died during succeeding epidemics and hunger; millions of people were displaced from their homes (Zagonjolli, M, Dam breaks Modeling, Risk Assessment and Uncertainty Analysis for Flood Mitigation, 2007).

The proposed Lower Awash dam is intended in Lower Awash River Basin just upstream of the Addis Ababa-Djibouti road main bridge on Logia River. Along with flood control, this proposed multipurpose dam will also be used to supply water for the proposed irrigation development farms in the Lower Awash plain.

In this study, a pre event breach analysis of the dam and mapping the downstream area inundated by the resulting catastrophic flood shall be conducted using HEC-RAS 5.0.3.

1.2 Problem Statement

Several problems could cause dam failure such as overtopping, piping, earth quakes, landslides etc. Consequently, by those reasons our world has experienced some catastrophic dam failures. Like the Shimantan dam that failed in 1975 killed an estimate of over one hundred seventy thousands of people and eleven million people becomes homeless in China; Machchu dam in 1979 killed 500 peoples in India; South Fork dam in 1889 killed 2209 people in United State and Vajont dam in 1963 over 2000 peoples are died in Italy (J. Andrew Chrles, 2011). As dams lead to a serious threat to peoples and infrastructures downstream of the dam, it has always been vital to analyze the causes and outcomes of catastrophic dam failure.

In Ethiopia construction of dams has boosted in recent years after many large dams have been built and several are under construction. Their purpose comprises flood regulation, development of irrigation, hydropower, water supply, or the combination of all these functions. Succeeding the formation of dams, the downstream ecosystem is highly transformed that massive area is being covered by irrigation farms, agro processing plants such as sugar factory are erected, new settlements and living areas of residents found on the farms and factories are established. All these investments and recently settled inhabitants are greatly unprotected to flooding and are at risk for damage and death respectively. Though no records are presented on dam breaches and the catastrophic damages they cause in Ethiopia, it is apparent to do a pre event analysis on dam breach and identify the flood affected areas.

This pre event dam breach analysis is therefore aimed to analyze the possible breaching process of the Lower Awash embankment dam and to delineate the area that would be flooded out due to the hazardous wave front.

1.3 Research Questions

1) What are the possible causes of the dam failure?
2) What are the hydraulic breach parameters defining the cross section of the failures?
3) What is the magnitude of breach outflow hydrograph?
4) What areas are covered by the flood?

1.4 Objective of the study

1.4.1 General Objective

The general objective of this study is to model the dam breach process, apply it to the case of Lower Awash dam and map the downstream area to be inundated by the flood.

1.4.2 Specific Objective

The specific objectives are:

1) To identify the possible mode of failure
2) To determine the dam breach parameters
3) To compute the breach outflow hydrograph
4) To prepare map for the inundated area

1.5 Scope of the Study

The scope of the study is extended to area in the flat plains downstream of Lower Awash dam. In this study the analysis is proposed on the prediction of breach outflow hydrograph for piping mode of failure. Among different dam breach modeling methods, HEC-RAS version 5.0.3 was used to estimate breach outflow and dam breach parameters. The flood inundation map has been prepared on RAS Mapper which is GIS tool of the HEC-RAS version 5.0.3 and by exporting the tiff raster file to ArcGIS. A trial version of ArcGoogle was also used to display important towns, roads and settlement areas that would be affected by the flood.

1.6 Significance of the Study

The output from the study of the Lower Awash embankment dam breach analysis will gives an effective and quick action plan that requires accurate prediction of inundation levels and inundation coverage. Thus the results of the study are important for the following reasons:

- ✓ Alert concerned government bodies to take a precaution on dam safety plans
- ✓ Prepare an early flood warning system
- ✓ Timely aware downstream inhabitants about the hazardous flood and
- ✓ Plan a proper emergency evacuation method on disaster time.

1.7 Structure of the Thesis

The study consists of five chapters. The first chapter is the introductory part which discusses the background, problem statement, research questions, objectives of the study, scope of the study, and significance of the study. On the second chapter the reviews of important literatures of the work are discussed. The third chapter discusses the methodology and general procedures used to achieve the study and gives detail descriptions on the study area including location, climate, hydrology, topography, and land use; moreover characteristics of the dam and reservoir under analysis are also discussed in this chapter. The outcomes of the study are discussed in chapter four. The last chapter concludes the study with the points of recommendation. Finally the list of references and appendix are annexed.

CHAPTER TWO

2. LITERATURE REVIEW

2.1 General Overview of Dam Breach

The breach of embankment dams is the action of eroding the embankment materials by flow of water either over or through the dam or beneath the foundation. The earlier results to overtopping of the dam and the succeeding external erosion; the second tends increase to internal erosion (Limin Zhang, Ming Peng, Dongsheng Chang, and Yao Xu, 2016). Although the word dam breach analysis usually associates to the process of studying a dam failure phenomenon and investigating the consequential effects at downstream region. Researchers have been working to develop computer programs that would help to design new dams or evaluate existing dams. In this part different literatures works including recent scientific journals, guidelines and books related to history of dam breach, dam breach modeling and breach parameter estimation methods, will be reviewed widely consistent with the new and efficient dam breach guidelines.

2.1.1 Review of Dam Breach Analysis Studies

Journal of River Engineering, (2014) by Saqib Ehsan and Walter Marx studied a dam break modeling for large earth and rockfill dams. In the study, Mangla dam, placed on Jhelum River in Pakistan, has been occupied into thought. This dam is among the major earth and rock fill dams found in the world with a height of 125 meters. By the use of MIKE 11 dam break component the erosion based overtopping break of the dam with raised situations has been investigated. To calculate the breach dimensions and model the breach development as a linear process the parametric way has been done to define the breach outflows. The breach outflow hydrographs was estimated for various breach modes. Additionally, the failure time and the breach destruction degree have also been calculated for measured breach cases. The maximum outflow for the worst occasion of dam break is about 160,000 cumecs which is near 2.5 times the extreme design flood for the dam. For prevailing & intentional dams found in the world, this model should be valuable for the dam breach study and the risk valuation purposes.

On journal of water and land development, (2016) by Boussekine M., and Djemili L; simulating technique for gravity dam failure examination was studied. This study grants an examination of dam break model of Hammam Grouz schemed in Algeria, to return flood with the dam break occurring near the peak of the flood occurrence. HEC-RAS was modeled to calculate water-surface profiles and dam break situations for the inflow design floods that were computed. For the area downstream inundation maps were established. The Rhumel Valley for 23 kilometers length downstream of the dam has been characterized in the model by regularly used interval of cross sections. The roughness coefficients as 0.033 and 0.05 for the river and over bank have been chosen respectively. The respective charge loss coefficient values of 0.3 and 0.1 associated with expansion and contraction of the channel, or related to natural problems, are comprised in the model. HEC expected the combined properties of reservoir inflow quantity, storage characteristics and the downstream valley backwater on the magnitude and the shape of the dam breach wave for the simulation work. The main sources of the flood analysis procedure are depth combined conservation of mass and momentum balance equations called shallow-water equations. A nearly exact hydrograph was produced from the model computed water surface elevations and flood hydrographs, using a calculation interval of two minutes. It was concluded that shorter time interval would yield somewhat well precise hydrograph, but also a very large amount of data, while a slightly fewer precise hydrograph would gained from a longer time interval. To properly warn the communities live in Oued Athamnia and Ain Smara Cities from affecting due to these flood damages, susceptibility plots are completed.

From international journal of engineering and technology, (2017) two dimensional dam break flow study for Ujjani dam was performed. In this study using Pandharpur city as learning extent, dam break flood routing is performed by the use of HEC-RAS two dimensional modeling for Ujjani dam for calculating flood vulnerable area at the downstream side of dam. Here the 2D flow area boundary and storage area boundary were clear and then mesh development was made after developing the terrain model. By implicit finite volume algorithm and wave diffusion equations unsteady flow modeling practiced. Unsteady flow study is performed out for dam break work; hydrograph output interval used as an hour, calculation interval taken 15 sec. According to the study report Ujjani dam will fail at adjacent flow discharge of 41,000 cumecs.

A study conducted by Bagus Pramono Yakti (2018), presented on web conferences about the two dimensional modeling of flood propagation due to the break of Way Ela dam sited in Negeri Lima Village, Leihitu District, Ambon Island. Due to the breach of this dam there was a developed flood that harshly smashed homes and different communal services. A two-dimensional (2D) model of HEC-RAS was confined for computation of the flow. Analysis of land cover was done to get the runoff coefficient and manning's n values for the inflow discharge hydrograph. To attain the inflow discharge hydrograph as the input for reservoir routing the dam failure outflow, hydrological parameter was examined. To route the reservoir as the parameter of reservoir storage characteristic, reservoir bathymetry was studied. The parameter for dam characteristic and dam catastrophe situation, dam parameter was analyzed with the reservoir routing. In this study, through the statement that the failure was initiated by overtopping, a simulation was conducted for the dam failure based on earlier studies. The inundation area, depth, and arrival time are all the results from the study. Orthophoto data were used to verify the inundation area. It was found that very small relative errors intended for the two areas are realized. There are up to six meter of the inundation depth in the village that reaches close with the stated depth having the flood entrance time of a couple of two hours.

2.1.2 Review of Dam Breach Analysis Studies in Ethiopia

According to the report of Kamal Eldin Bashar M. K., (2005) in Ethiopia, traditional minor scale irrigation systems have existed centuries ago, particularly in the eastern, central, north western parts of Ethiopia for the irrigation and water supply purposes. According to the Nile Basin Capacity Building Network for River Engineering study, the diversion structures were made of wood, stones, and grass with earth. During high river flows they were frequently washed away and have to be reconstructed every year. Modern minor level irrigation using micro-dams were started following major droughts have affected the country in the year 1973/74 and 1984/8). However there are no histories on dam breach and its catastrophic damage triggered in Ethiopia, now a day significant number of studies on dam breach analysis, risk assessment and flood inundation mapping have been done by the researchers and design offices to give prior emergency action plans for those constructed as well as proposed dams. Some of the recent models and studies on dam breach analyses in Ethiopia are discussed below.

Abimael Leoul, (2015) studied a dam breach analysis for the case of Kesem Kebena Dam. Within this study overtopping and piping modes have been checked using one dimensional river analysis HEC-RAS model and empirical equations are used to calculate dam breach limits for his use in the model. From the dam up to the downstream boundary that is sixty kilometers from the dam, the modeling process was for performing unsteady flow calculations in the intent of routing the breach outflow downstream of the dam. The models HEC-RAS and HEC-GeoRAS were applied. The researcher stated that whether or not the peak outflow resulted by empirical formulas was related to peak outflow empirical equations and peak out flow envelop curve from exactly failed dams, MacDonald and Langridge-Monopolis (1984) was set to be well accurate as can be realized in the outcome. Peak outflow obtained using MacDonald and Langridge-Monopolis (1984) have inaccuracy of 0.3 when compared to peak outflow equations and places in the peak outflow historical curve. Similarly inaccuracy of 0.4 from peak outflow obtained by Froehlich (2008) was found as related to peak outflow empirical equations from historical failure and places outside the peak outflow envelop curve. Therefore, in this dam breach study the peak outflow obtained by MacDonald and Langridge-Monopolis was selected for extra unsteady flow study in HEC-RAS and inundation mapping.

Similarly, Adnan Arega, (2017) prepared dam breach analysis and flood inundation mapping for Koga dam which is found in the Tana sub basin of Abay Basin in Ethiopia. On his study the dam has been analyzed for overtopping and piping cases by means of HEC-RAS model, and defined empirical equations were used to forecast characteristics of dam breach for use in the simulation model. Resulting from the PMF the spill way structure could not be collapsed or miss-operated and breaking of the embankment will not expected in HEC-RAS, but piping failure was simulated in the model using breach parameters calculated from the empirical equations. The modeling development was set to perform unsteady flow calculations in the intent of routing the breach outflow downstream of the. This is extended to the downstream boundary about twelve kilometers far from dam. The models HEC-RAS and HEC-GeoRAS were used alternatively. The researcher founded and concluded that the breach peak flow estimated is about 3070 cumecs and an area of two hundred and eighteen hectare downstream of the embankment dam will be flooded due to the dam break.

Wubalem Tolosa, (2018) modeled a two dimensional dam breach for Gidabo dam due to piping failure on his MSc thesis dissertation to Addis Ababa Science and Technology University. In the study determination of the dam breach parameters, potential risks, safe settlement areas and finally preliminary arrangement of flood protection work was aimed predominantly. The researcher carried out the study in four steps. First, the breaching way was examined, the critical hydrological event was recognized, and four breach parameter estimators were analyzed, breach width of 97m, side slopes 0.7 (H:V), and breach formation time of 2.6 hrs were obtained. Afterward, a numerical simulation of the dam break flood was executed using HEC-RAS 2D modeling. Thirdly, according to flood modeling, flood hazard risk analysis was conducted and resulted that the peak discharge would be 8715 m3/s at the breach and 8622 m3/s near settlement area, at 2.6km away from the dam. The period when the dam break starts up to the arrival of peak discharge at these area is three hours. The flood map was produced to isolate society found at risk and safe settlement areas; consequently, a total of, 81% of the inhabited would be under flooding. Finally, from the study it was suggested that a principal arrangement of permanent flood control dike was recommended with a length of 1.25km and an average height of 15m that would make ninety eight percent of the settlement zone on the left side kept safe.

Haile Belay, (2018) unlike Wubalem Tolosa developed a 2D dam break modeling for Gidabo dam due to overtopping failure mode. Gidabo dam is one of such dams and provides flood control and irrigation water for sugarcane and rice. It is an earth fill dam having 25m height and 335m crest length with side ogee spillway to permit 10,000 years' flood. For this study HEC-RAS 5.0.3 was used to analyze the dam breach for overtopping failure. ARC-GIS and GIS tool of HEC-RAS called RAS Mapper were used to create flood inundation map. He calculated the dam breach parameters within the HEC-RAS model by using HEC-RAS beach parameter calculator tab. A 2D unsteady flow simulation of the dam breach was done by using the inflow hydrograph as upstream boundary condition. Breach parameters were 143m breach bottom width, 1.4 breach side slope and 2.7hr breach formation time as shown on his result. The expected peak breach outflow was 15848 cumecs which covers area of 2050 hectares. The flood map displayed that irrigation command area irrigated by the right side canal and peoples settled 4.5 km downstream of the dam were found to be adversely flooded.

2.2 Dam Failure Hazard Classification

According to the article on hazard potential classification system for dams prepared by the Federal Emergency Management Agency and Interagency Committee on Dam Safety, (2013); hazard caused by dam failure is classified in to the following four major groups.

a) High Hazard Dam
b) Significant Hazard Dam
c) Low Hazard Dam
d) No Public Hazard (NPH) Dam

a) High hazard dam

High Hazard Dam is a dam for which loss of human life is expected to result from failure of the dam. Designated settlements found downstream inside the boundaries of likely inundation could also be assessed for potential damage on human life. It is good to know that the likely of loss of an individual life is sufficient to categorize a dam as high hazard (Claudia C & Mark, 2010).

b) Significant Hazard Dam

Significant Hazard Dam is a dam where substantial harm is predictable to happen, but no damage of human life is anticipated from break of the dam. Significant damage can well-defined as risk to structures where people totally living, working, or recreating, or community or isolated services. Significant damage is defined to be damage enough to condense structures or services dilapidated or impracticable.

c) Low Hazard Dam

Low Hazard Dam is a dam where loss of human life is not probable, and substantial failure to structures and public services as stated for a "Significant Hazard" dam is not likely to hapen from break of the dam.

d) No Public Hazard (NPH) Dam

No Public Hazard (NPH) Dam is a dam where loss of human life is not expected, and that damages only to the dam proprietor's stuff can consequence from breach of the dam.

2.3 Dam Breach Mechanism

As stated by Yitbarek Kifle, (2016); dam break modelling and inundation mapping for Tendaho and Logia dams, breach forming mechanisms can be classified into two general categories.

2.3.1 Overtopping Failure of Earthen Dams

Overtopping occurs when the water surface elevation in the reservoir exceeds the height of the dam; water can then flow over the top crest of the dam, an abutment, or a low point in the reservoir rim. This typically comes from a design insufficiency of the dam/spillway arrangement and reservoir storage capacity to overcome the resulting flooding incident. When a reservoir's outlet arrangement is not working appropriately a failure may also occur, so increasing the water surface elevation of the dam. A dam failure resulting from an embankment slide can also lead to an overtopping failure when the slide encroaches upon the high water line. The most usual failure type for embankment dams is overtopping as a result of flooding.

2.3.2 Piping and Internal Erosion of Earthen Dams

Internal erosion and piping happens after concentrated seepage progresses within an embankment dam. Large voids in the soil are produced as the seepage gradually erodes the dam. Naturally, piping initiates close the downstream toe of the dam and undergo its way to the upper reservoir. Erosion becomes quicker as the voids become wider. Water flow through the embankment will look muddy as erosion grows. The piping hole can increase and cause the dam crest to failure once the erosion reaches the reservoir. Piping catastrophes are basically modeled in two cases, before and after the dam crest ruins. Water discharging inside the piping hole is modeled as orifice flow before the dam crest fails and as weir flow after the dam crest fails. For minor dams built from consistent soils, it is likely for the reservoir to fully empty earlier the dam crest breakdown. Mostly, internal erosion brings comparatively more number of the earthen dam failures. As related with the external erosion, it is an extended term procedure and many influences occurred. Irregular upsurges of outflow discharge and leakage of disorganized water are the visual suggestion of continuing erosion. In some suitcases, internal erosion and piping may happen likely since the persuaded force will be mutual for both that found from the water flow with larger hydraulic gradient.

2.4 Dam Breach Parameters

Limin Zhang, Ming Peng, Dongsheng Chang, and Yao Xu, (2016) described that the term dam breach parameters will contain the parameters required to physically define the breach. Such breach parameters could be separated into two groups, i.e. geometric and hydrographic. An embankment dam breach often has a trapezoidal shape, with the geometric parameters of breach depth, breach top width, average breach width, breach bottom width, and breach side slope factor. Any combination of three of the five geometric parameters defines the breach shape and size. Peak outflow rate and failure time are among hydrographic parameters.

Moreover, Wurbs, (1987) stated that it is needed to make consistent estimations of peak outflow and the resulting downstream inundation in close nearness to the dam by performing accurate prediction of breach parameters. In huge reservoirs, when the breach extents its supreme depth and width the peak discharge happens; changes in reservoir head are relatively slight during the breach formation period. In these cases, exact prediction of breach geometry is most important. For small reservoirs, there is substantial variation in reservoir level during the formation of the breach, and as a result, the peak outflow occurs before the breach has fully developed. So it is reasonable that the breach formation frequency is a key parameter.

2.5 Overview of Dam Breach Models

As discussed on FEMA (2013), dam breach models can be one dimensional or two dimensional. One-dimensional models solve either full dynamic or simplified forms of one-dimensional, cross-section averaged shallow water equations. These models are more complicated than simplified numerical models and do basically focus backwater effects; and one-dimensional models are capable of dynamic reservoir routing rather than level pool routing. One- dimensional routing is impartially sophisticated, but is best suitable for modeling flow through well- defined, confined channel. Two-dimensional models use full dynamic or simplified forms of one-and two-dimensional shallow water equations to solve both one-dimensional channel flow and two-dimensional overland flow. Two-dimensional models are capable of routing flow over unconfined floodplains where flood waters are not contained within a defined channel. Dam breach modeling can be divided into two types.

According to FEMA, (2013) the modeling methods can be:

- ✓ Tools that generate the dam breach peak discharge and hydrograph only
- ✓ Tools that develop a breach hydrograph and perform downstream flood routing using a one-or two-dimensional hydraulic model

Table 2. 1: Most widely used dam breach modeling tools (FEMA, 2013)

Method	Peak discharge generation	Breach parameters	Breach hydrograph	Downstream routing capability			
				steady state	Unsteady state	1D	2D
breach hydrograph generation only							
Empirical Equations	X	X					
NWS BREACH	X	X	X				
USACE HEC-1 and HEC-HMS	X		X	Without downstream hydrologic routing	X		
One-dimensional models							
WinDAM		X	X				
NWS SMPDBK	X			X		X	
NWS FLDWAV	X	X	X		**X**	X	
USACE HEC-1 and HEC-HMS	X		X	Downstream hydrologic routing	X	X	
USACE HEC-RAS	X		X	X	X	X	
Two-Dimensional Models							
MIKE© FLOOD	X		X		X	X	X
HEC- RAS 5.0.3	X	X	X	X	X	X	X

2.5.1 Dam Breach Model Selection Criteria

In recent years, according to World Metrological Organization, (1994) flood inundation models become important progressively in both flood forecasting and damage valuation as it affords the basis for the decision making of flood risk management. Such models are mainly used to simulate flood inundation extent and depths at different sections of the studied flood rivers. The selection of particular model is a key issue to get acceptable answers to a specified problem. Currently, there are many hydraulic and hydrologic models available to simulate the hydraulic and hydrologic processes at spatial and temporal scale. Though, there is no clear standards for making a choice between models, some simple guideline can be specified. Some of the factors and criteria involved in the selection of a model include the importance of the required model out puts, availability and quality of the input data, the hydraulic and hydro geological characteristics of the basin, the availability and size of computers for model development and operation.

Two-dimensional models use full dynamic or simplified forms of one-and two-dimensional shallow water equations to solve both one-dimensional channel flow and two-dimensional overland flow. Two-dimensional models are capable of routing flow over unconfined floodplains where flood waters are not contained within a defined channel. According to FEMA (2013), the selection of an appropriate model for computing a dam breach outflow is dependent on:

- ✓ Type of results needed,
- ✓ The level of effort that can be expended, and
- ✓ The potential for loss of human life and economic damages that can result from the dam failure.

Table 2.2 presents FEMA (2013) guidance to determine the level for analysis for dam failure and appropriate dam breach modeling methods.

- ✓ Level 1 and level 2 analyses are most appropriate for low-hazard potential / small sized dams with dam height (10-40m) and significant-hazard potential / intermediate-sized dams with dam height (15-40m).
- ✓ Further detailed surveying or modeling shall be used for level 3 analyses for high-hazard potential / large-sized dams with dam height greater than 40m.

Haile Belay, (2018) from the literatures worked on dam breach analysis in Ethiopia found that the model selection was performed based on the hazard potential of the dam. For dam under large sized class HEC-RAS 5.0.3 two dimensional unsteady flow model was selected for breach parameters prediction, breach outflow hydrograph generation and downstream flood routing for Gidabo Dam breach analysis and flood inundation mapping.

Table 2. 2: Recommended dam Breach analysis methods (FEMA, 2013)

Level	**Applicable To**	**Breach Parameter Prediction**	**Peak Breach Discharge Prediction**	**Downstream Routing of Breach Hydrograph**
Level-I (Simple Analysis)	Low-hazard potential / small size	Empirical Equations	SMPDBK, Geo Dam-BREACH, HEC-HMS	GeoDam-BREACH, SMPDBK, HEC-HMS
Level-II (Intermediate)	Significant-hazard potential / intermediate size	Empirical Equations	HEC-HMS or HEC-RAS Unsteady Model	HEC-RAS (Steady or Unsteady Modeling) 1-D or 2-D models
Level-III Advanced	High-hazard potential / large size dams with sufficient population at risk to justify advanced analyses	Empirical Equations, NWS BREACH, or WinDAM	HEC-RAS Unsteady Model	HEC-RAS Unsteady Model or 2-D models

2.6 HEC-RAS Model

According to USACE, (2010) it has confirmed very useful in supporting all stages of river control planning due to its ability of describing that diverse variety of physical developments. HEC-RAS enables both overtopping and piping failure approaches with the failure start being a target water surface, water surface and duration, or specific time. To analyses a dam breach in RAS, enters the failure type, break size, and break time. The breach size is demarcated by a trapezoid and the period over which the breach happens. Finally, RAS helps the modeler to modify the development of the breach over the full formation time. Basically, the software has four 1D river analysis components: steady flow water surface computations; unsteady flow simulation; sediment transport computations; and water quality analysis. HEC-RAS also has a quite a number of options, such as mixed flow regime analysis, allowing analysis of both sub- and supercritical flow regimes in a single computer run, culvert and bridge routines allowing for multiple openings of different types and sizes, quasi 2-D velocity distributions, and xyz graphs of the river channel system. The stream flow profile follows the basic physical laws: principle of conservation of mass and principle of conservation of momentum. These laws are expressed mathematically and referred as continuity and momentum equations. In unsteady flow, time dependent changes in flow rate are analyzed explicitly as a variable, while steady flow analysis models neglect time all together.

As stated by HEC-RAS 2D user's manual, USACE (2016), HEC has added the capability to do two dimensional hydrodynamic simulations inside the unsteady flow analysis portion of HEC-RAS. The user nowadays perform one-dimensional unsteady flow modeling, two-dimensional unsteady flow modeling (Saint Venant equations or diffusion wave equation or diffusion equations), as well as combined 1D and 2D unsteady flow routing. The two dimensional flow areas in HEC-RAS can be used in a number of ways. Two dimensional unsteady flow modeling is worked by putting 2D flow area fundamentals in to the model in the similar manner as adding a storage area. A 2D flow area is added by drawing a 2D flow area polygon; developing 2D computational mesh; then linking the 2D flow areas to the storage area. The dam can be modeled as storage area and 2D flow area connection. However, this study was conducted by a two dimensional unsteady flow modeling using HEC RAS model.

2.6.1 Reservoir Routing for Dam Breach Modeling in HEC-RAS

From the study by Chris Goodell; WEST Consultants, (2015) HEC-RAS software can route flows through the reservoir before, during, and after the dam breach event with any of the following three methods:

a) **Level Pool Routing**: The discretized form of the continuity equation and an analytical or empirical relationship between stage or storage in the reservoir and discharge at the outlet of the reservoir.
b) **One-Dimensional Dynamic Routing:** The full dynamic wave form of the St. Venant partial differential equation of conservation of momentum combined with the continuity equation in the streamwise direction. Discretized forms of the St. Venant Equations are used to solve for Stage and Flow at each cross section simultaneously for each time step.
c) **Two-Dimensional Dynamic Routing:** The full dynamic wave or diffusive wave form of the St. Venant partial differential equation of conservation of momentum coupled with the continuity equation in two dimensions (the x-y plane). Discretized forms of the St. Venant equations are used to solve for Stage and Flow at each cell in a 2D mesh.

2.6.2 HEC-RAS Model Calibration

After new study by Habtamu Tamiru, (June 2019) calibration is the modification of the model's parameters such as channel roughness, and hydraulic structure coefficients, so that it reproduces practical measured data to a satisfied accuracy. For development of hydraulic models for the dam breach flood calculating and flood inundation mapping channel roughness is defined as the most important parameter. Hence, it is vital to calibrate the channel roughness coefficient (Manning's "n" value) for several points in the 2D flood area through model of floods. If observed or measured historic data such as flow hydrograph, water level, water depth, flood extent of the event study are accessible during flood occasion, it can be simple to calibrate HEC-RAS outcome of flooded map, if all the above data are lost or not existing, situations may be hard in both cases. Hence, the modeler is required to check trial and error to change manning roughness coefficient for calibration till the simulated stage or flow hydrograph come from HEC-RAS and the detected stage or flood hydrograph occasion come to be alike.

2.7 Flood Inundation & Flood Hazard Mapping

As stated by the report on ICOLD, (1998) inundation maps display spatial magnitude of the flood contour for different states of certain return periods, in most cases up to PMF, and flood contours of possible dam break floods produced by a "sunny day failure" and a failure overlaid on certain natural "base flood circumstances". Flood hazard region in the river basin defined by the inundation or hazard valuation mapping participating native information, hydrological, meteorological and geomorphologic figures using different methods. According to FEMA, (2013) inundation maps can have a different uses including emergency action plans, mitigation planning, emergency response, and consequence assessment.

Central Water Commission, (2018), Guidelines for Mapping Flood Risks Associated with Dams, defined flood hazard as a sign of the possible source of threat due to flooding. These, however, does not suggest any risk unless persons or objects that are susceptible to destruction are exposed to it. Flood hazard diverges with flood harshness (i.e. for the similar location, the bigger the return period of the flood the more severe the hazard) and place inside the floodplain for the same flood incident. This varies with both flood behavior (velocity and depth, the rate of rising of floodwater and the time from rainfall to flooding) and the interface of the flood with the topography. The hazards to be mapped consist of themes such as the flood inundation areas, water depths and velocities, and arrival times of flood waves.

For this study most recent literatures including articles and research works that were studied all round the world and particularly in Ethiopia on dam breach analysis, flood risk assessment and inundation mapping have been reviewed. Most of the previous works are one dimensional dam break modeling whereas now a day a two dimensional unsteady flow modeling using the hydrologic engineering center river analysis system HEC RAS have been performed by different scholars and researchers. However, this study focuses on breach analysis for piping failure by using the HEC-RAS two dimensional unsteady flow modeling.

CHAPTER THREE

3. METHODOLOGY

3.1 Description of the Study Area and Dam under Analysis

3.1.1 Location

The Lower Awash Dam and Irrigation Development Project are located in Zone 1 and 4 of Afar National Regional State, at about 700 km northeast of Addis Ababa. The proposed multipurpose dam is located on Logia River approximately about 100km upstream from the bridge on Logia River of main road to Djibouti. The command area of the project lies on left side of the Logia River. Basin wise, the project is located in Awash River Basin with geographic coordinates of the proposed dam site is 1308800 UTM Northing and 652575 UTM Easting. The location map of project area is presented on Figure 3.1 below.

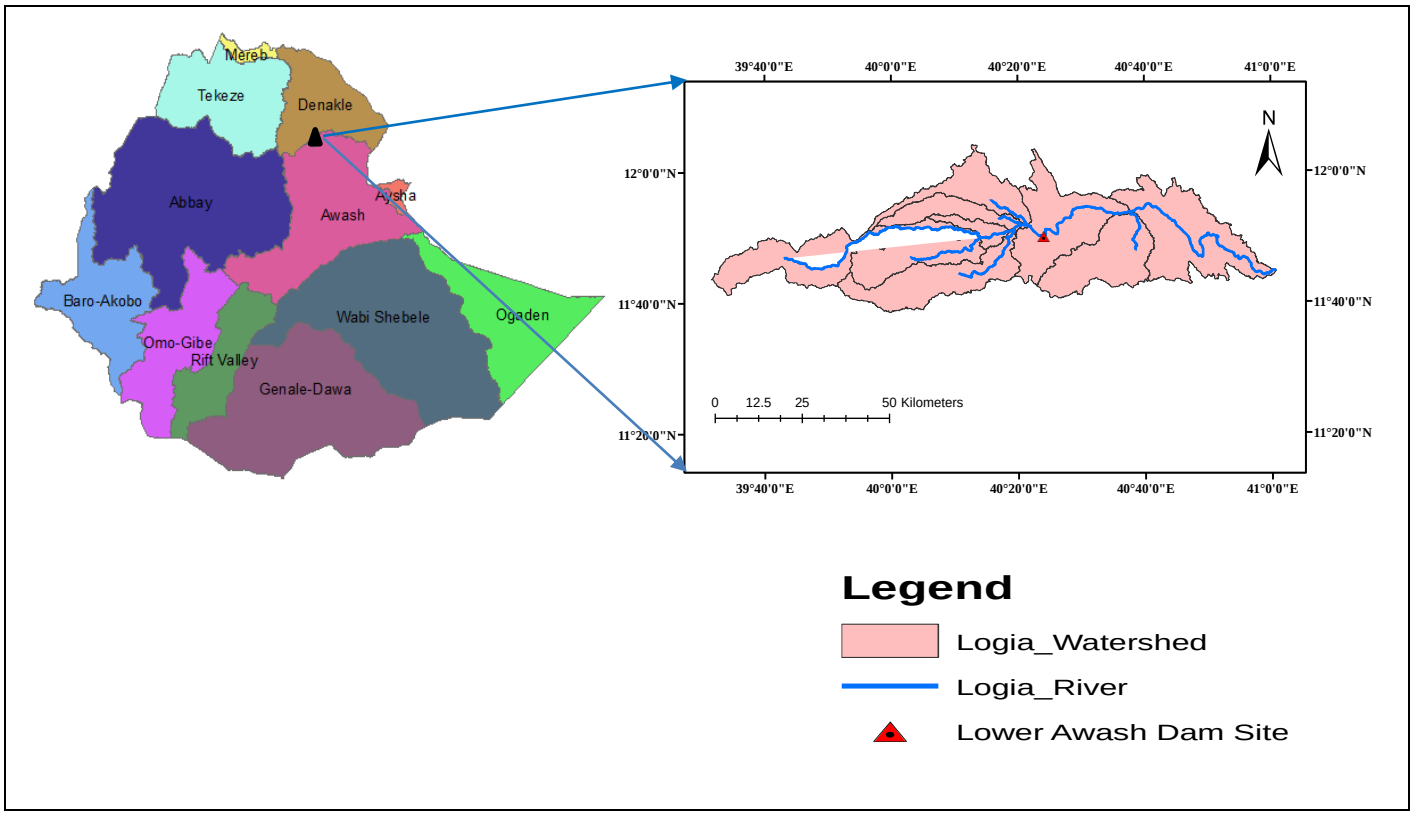

Figure 3. 1: Location Map of Lower Awash Dam and Irrigation Project Area

3.1.2 Climate

Rainfall

There are few meteorological stations around the catchment with different length and type of record mainly concentrated in the upper, lower and southern boundary nearby catchments, although there is none within the catchment. The rainfall of all the nearby stations was considered for analysis. Some of the rainfall stations considered for the catchment area are Weldiya, Bati, Mersa, Mille and Dubit gauging stations. About 80% dependable rainfall is adapted as consistent with the national experience and the extreme variability nature of the rainfall. The dependability of rainfall in January and February, October to December is almost none and the agricultural production has to fully utilize irrigation water as far as agriculture is concerned; Lower Awash dam and irrigation development project study and design final feasibility report (WWDSE, 2016).

3.1.3 Hydrology

From WWDSE, (2016) Lower Awash dam and irrigation project hydrology report the Awash drains the northerly part of the Rift Valley in Ethiopia from approximately 8.5 ºN to 12 ºN with total drainage area of 112, 696 square kilometers. The source of the Awash lies at an altitude of around 2500 meter above sea level in plateau to the west of Addis Ababa. It first flows east, draining the Becho plains and is joined by several small tributaries before entering Koka Reservoir. After being released through Koka Dam, which came into operation in 1960, it descends into the Rift Valley. The fall of the river in this reach is used for hydropower generation at Koka and series of run-of river schemes designated as Awash II and Awash III. The river then turns gradually northwards, flowing at much-reduced gradient along the base of the western highlands. In the reach between Koka and Awash Station, the Awash River is joined by small tributaries like Keleta, Wererso and Arba draining the highlands, which define the catchment boundaries to the east. Beyond the Awash Station, the Awash Basin expands into the eastern plains w the Rift valley widens. Although the eastern plains account for some 40% of the area of the Basin, its drainage channels terminate before reaching the Awash and also receive low rainfall, less than 600 mm per year.

Between the Awash Station and the Gedebassa swamp (Hertale Station) major tributaries, the Kesem and the Kebena, enter the Awash originating from western highlands after passing through deeply incised gorges. From the eastern side the Herdini River joins the Awash. From the Hertale Station to the Tendaho Station Ataye, Borkena, Chelela and Mille rivers originating from Wollo highlands joined the Awash River in this reach contributing about 900 MCM of water annually. The hydrological regime at this reach is complicated by major losses in the Gedebassa swamp complex. Estimated losses vary from 400 MCM to 2900 MCM per year.

3.1.4 Dam and Reservoir Characteristics

As obtained from the study and design of Lower Awash dam and irrigation project final feasibility report, (WWDSE, 2016) Lower Awash dam is a Zoned Earth-Rock fill dam having central clay core with crest length of 335m and crest width of 10m. Its height is 48m having the dam crest level at 771 m and river bed level at 723m. m.a.s.l; the upstream slope is 1V:2.5H whereas downstream slope is 1V:2.25H. The reservoir is intended to accommodate a total of 470 million cubic meter of water, covering a total surface area of 60 square kilometer. As per the hydrological study report the 10,000 years return period inflow flood is 1971m3/sec whereas PMF is 3120m3/sec. The half PMF being 1560m3/sec is found to be less than 10,000 years return period flood, therefore, 10,000 years return period flood has been used for the design of spillway and PMF has been used to check the freeboard of the dam and its appurtenant structures. The spillway is ungated type having a total length of 30m.

3.2 Conceptual Framework

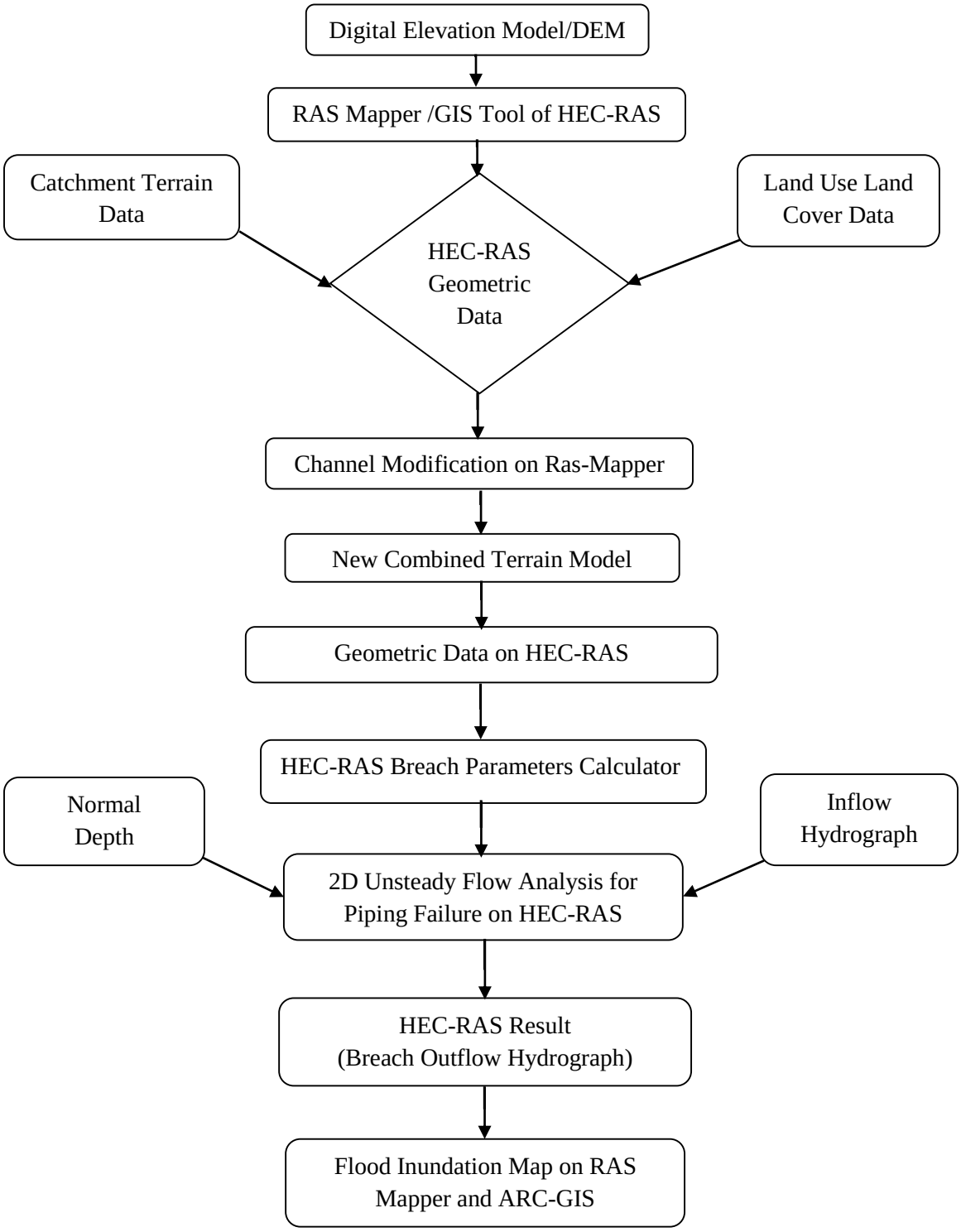

Figure 3. 2: Conceptual Framework

3.3 Data Collection

The necessary data used to perform this study were collected from different sources. Some of these data were terrain data and land use/land cover data of the catchment, original ground level data along the axis of Lower Awash dam, dam and spillway profile characteristics, and reservoir characteristics. The original ground level data were collected from detailed survey of the Logia River along the axis of the dam. The land use/Land covers of the catchment, DEM 20m resolution and soil data were collected from GIS department of Ministry of Water, Irrigation and Electricity. Land cover data of the area downstream of the dam was collected from the field visit survey and the latest land use land cover map of Awash sub basin, then verify it from relevant literature Chow (1959), whereas the reservoir and dam characteristics were obtained from Water Works Design and Supervision Enterprise (WWDSE, 2016), the study and design of Lower Awash dam and irrigation project final feasibility report.

3.3.1 Hydrologic Data

The inflow hydrograph which is a primary input for a 2D unsteady flow analysis as an upstream boundary condition were obtained from Lower Awash proposed dam and irrigation project hydrology report (WWDSE, 2016) analyzed from the stream flows of different periods collected at Logia gauging station near Logia town.

3.3.2 Hydraulic Data

Manning's roughness coefficient, (N) values used to describe the 2D flow area roughness or resistance to flow were determined using methods from Chow (1959) in relation with the result of the geometric data processor as the 2D flow area was classified in to different land uses developed by the Ras mapper tool of HEC-RAS 5.03, which is shown on appendix E & F.

3.3.3 Dam and Reservoir Data

Dam and reservoir data which includes the cross-sectional profile of the dam body and its spillway, the original ground level data along the axis of the dam, and the Capacity-Elevation Curve of Lower Awash reservoir were obtained from Water Works Design and Supervision Enterprise (WWDSE, 2016) design document of Lower Awash Dam and Irrigation project feasibility report, which is shown on appendix A & C.

3.4 Data Analysis

3.4.1 Filling Missing Rainfall Data

The data series obtained from the stations contains enormous missing data inside the record. Different techniques have been employed to fill the data gap. When there are concurrent data in the surrounding stations, the Inverse Distance Square method technique is used to fill the missing data using at least three stations. In some instances, it may be found that, data is missing in all the surrounding stations and inverse distance square method is no longer valid. In this case, the anticipated value of the rainfall series could statistically represent any one of the missing data at that particular decade and is filled with such values.

$$P_x = \sum_{i=1}^{n} \frac{P_i / D_i^2}{1 / D_i^2} = \frac{\frac{P_1}{D_1^2}+\frac{P_2}{D_2^2}+\cdots+\frac{P_n}{D_n^2}}{\frac{1}{D_1^2}+\frac{1}{D_2^2}+\cdots+\frac{1}{D_n^2}} \quad \text{(3.1)}$$

Where, P_x an index station that contains the missing data, P_i's are the concurrent value of rainfall at the surrounding stations and D_i^2's are the distance between P_x and the surrounding station.

3.4.2 Checking Consistency and Adjustment of Rainfall Stations

Where the characteristics of the record have not altered by time the record can be said consistent. Adjusting for gage consistency involves the estimation of an effect rather than a missing value. The consistency of rainfall records on selected stations commonly checked by double mass curve analysis. Double mass curve is a graphical method for identifying and adjusting inconsistency in a station record by comparing its time trend with those of adjacent stations. Irregularity would rise in the rainfall data of that station when the situations related to the recording of a rain gauge station have experienced a major change through the time of measurement. This inconsistency can be differentiated from the time the significant change took place. If significant change in the regime of the curve is observed, it should be corrected by using the following equation.

$$P_{cx} = \frac{P_X M_c}{M_a} \quad \text{(3.2)}$$

P_x and P_{cx} are original recorded precipitation and modified precipitation at any time period, whereas M_a and M_c are original slope and modified slope of the double mass curve respectively.

3.4.3 Estimation of the Probable Maximum Precipitation

According to WMO (1986) PMP which helps for calculating PMF is the largest depth of precipitation for a certain period that is physically probable in a particular area and topographical location at a certain period of the year. WMO (1986) suggested Statistical procedures for estimating probable maximum precipitation wherever sufficient precipitation data are available as presented below:

a) Extraction of maximum annual daily rainfall for 47 years from the daily rainfall data for Batti, Dubti, Mersa, Mille and Woldya stations.

b) Calculating PMP of the individual stations by using Hershfield (1965) formula.

$$X_{PMP} = X + \sigma K_m \quad \text{..... (3.3)}$$

Where, X_{PMP} is PMP estimate for a station, X stands for mean of the annual extreme series, σ is the standard deviation of the annual extreme series and K_m corresponds to frequency factor.

Frequency factor 'Km' is obtained by equation 3.4.

$$K_m = \frac{X_{max} - X_{n-1}}{\sigma_{n-1}} \quad \text{..... (3.4)}$$

Where, Xmax is the largest value of the annual extreme series, Xn-1 is mean of the annual maximum series omitting the largest value from the series, and σ_{n-1} is standard deviation of the annual extreme series omitting the largest value from the series.

c) Determine area PMP by using Theisen's polygon method using the formula:

$$Areal_{PMP} = \frac{A_1 PMP_1 + A_2 PMP_2 + \cdots + A_n PMP_n}{A_{Total}} \quad \text{..... (3.5)}$$

Where, PMP_1, PMP_2, PMP_n are probable maximum precipitation at station 1, 2, and n respectively, and A_1, A_2, A_n are Thiessen polygon areas of station 1, 2, and n respectively.

d) Hershfield formula for PMP is valid only for area less than 25 square kilometer. For areas greater than 25 square kilometer area reduction factor must be applied. For Ethiopia area reduction factor is not calculated. For large watershed, greater than one thousand square kilometers, area reduction factor lower than 0.6 have been used in East Africa (Watkins and Fiddes, 1984). For this study 0.59 is used as a reduction factor.

3.4.4 Inflow Hydrograph

In dam breach analysis inflow hydrograph is required as upstream boundary condition. In this study, the inflow hydrograph of the proposed Lower Awash dam site was computed by using the standard dimensionless SCS unit hydrograph for the computed probable maximum precipitation. Soil Conservation Service (SCS) dimensionless unit hydrograph is broadly used for hydrologic project. This technique uses a dimensionless unit hydrograph, with the flood area, the depth of the runoff capacity, the time-to-peak, and the SCS peak rate factor. The standard SCS-CN method is according to the following relationship between rainfall, *P* (mm), and runoff, *Q* (mm) (Schulze et al. 1992).

$$Q = \frac{(P-0.2S)^2}{P+0.8S} \quad \text{..... (3.6)}$$

Where *S* (mm) is potential maximum retention after runoff begins, which varies with antecedent soil moisture and other variables, can be estimated as:

$$S = \frac{25400}{CN} - 254 \quad \text{..... (3.7)}$$

Where, CN is runoff curve number

3.4.4.1 GIS Based SCS-Curve Number Determination

In Soil Conservation Service (SCS) method curve number determination is the most significant task. CN is a dimensionless catchment parameter reaching from 0 to 100. A CN of 100 characterizes a warning condition of a perfectly impervious watershed with zero retention, in which all rainfall becomes runoff. A CN of zero conceptually represents the other extreme, with the catchment extracting all rainfall and with no runoff regardless of the rainfall amount. The curve number can be calculated from experiential data. The SCS has established typical tables of curve number values as functions of watershed land use/land cover situations and hydrologic soil group (SCS-USDA, 1986)

The HSG refer to the standard SCS soil classifications ranging from A, which refers to sand and aggregated silts with high infiltration rates, to classification D, which corresponds to soils that swell significantly when wet and have low infiltration rates. The HSG reflects a soil's permeability and surface runoff potential.

For a catchment with sub-areas that have different soil types and land use, a composite curve number CN_c is determined by weighting the curve number values for the different sub-areas in proportion to the land area associated with each:

$$CN_c = \frac{CN_1A_1+CN_2A_2+CN_3A_3+\cdots CN_iA_i}{A_1+A_2+\cdots+A_n} \quad \text{(3.8)}$$

Where, CN_i is the curve number of the sub-area i, A_i is the area of the sub-area i, and n is the total number of sub-areas.

For this study methodology for SCS-CN determination was GIS-based. Land use/land cover and soil type shape files were first obtained and compiled in a GIS. Soil and land use shape files were intersected using GIS techniques, to generate new and smaller shape files associated with the hydrologic soil group and land use names. This step keeps all the details of the spatial variation of soil and land use. The curve number data base was built based on the intersected land soil layer and its related attribute table. Finally the runoff curve number was determined by using soil conservation service tables. Figures 3.3 & 3.4 below present the land use land cover and soil group of the study area respectively.

3.4.4.2 Parameters of the Inflow Hydrograph

To determine the inflow hydrograph of the catchment the drainage network above the dam site have been delineated from the 20m DEM using Arc SWAT tool in the GIS. The GIS processing phase includes derivation of the important morphological characteristics that is used to derive the maximum time of flow concentration (tc), the longest flow length (*L*), the centroidal flow length (Lc) and the average slope.

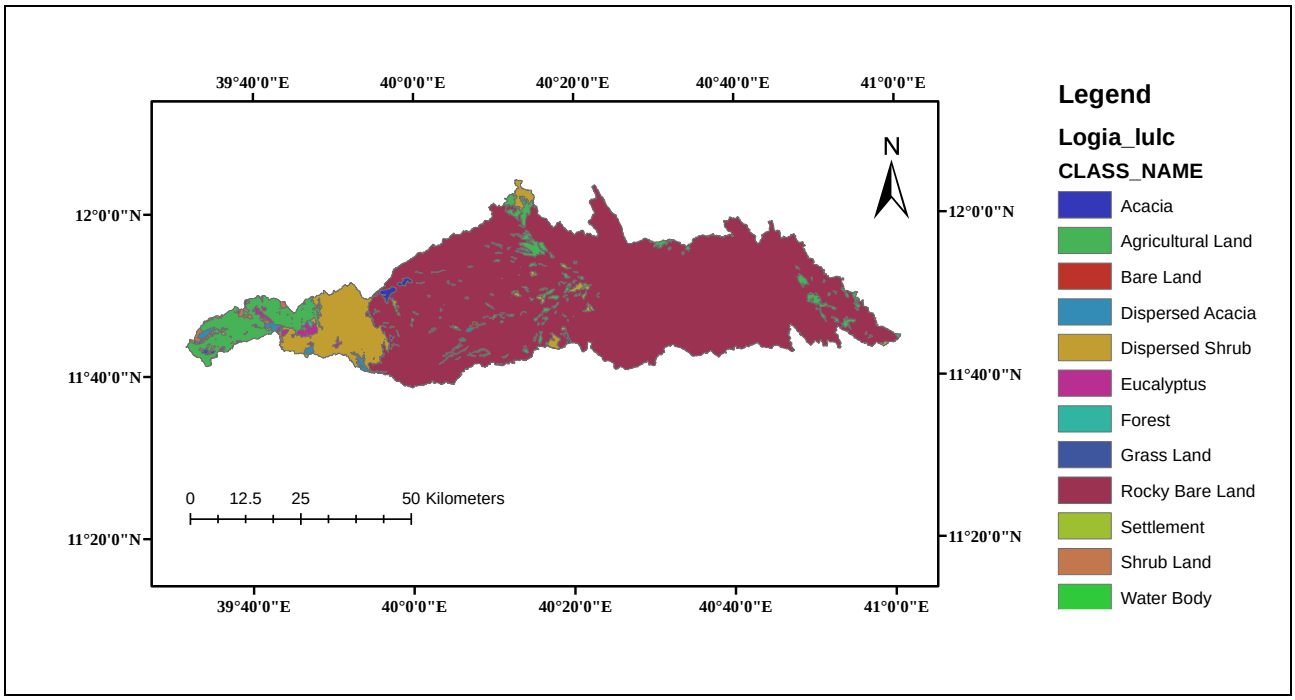

Figure 3. 3: Logia Watershed Land Use/Cover Map

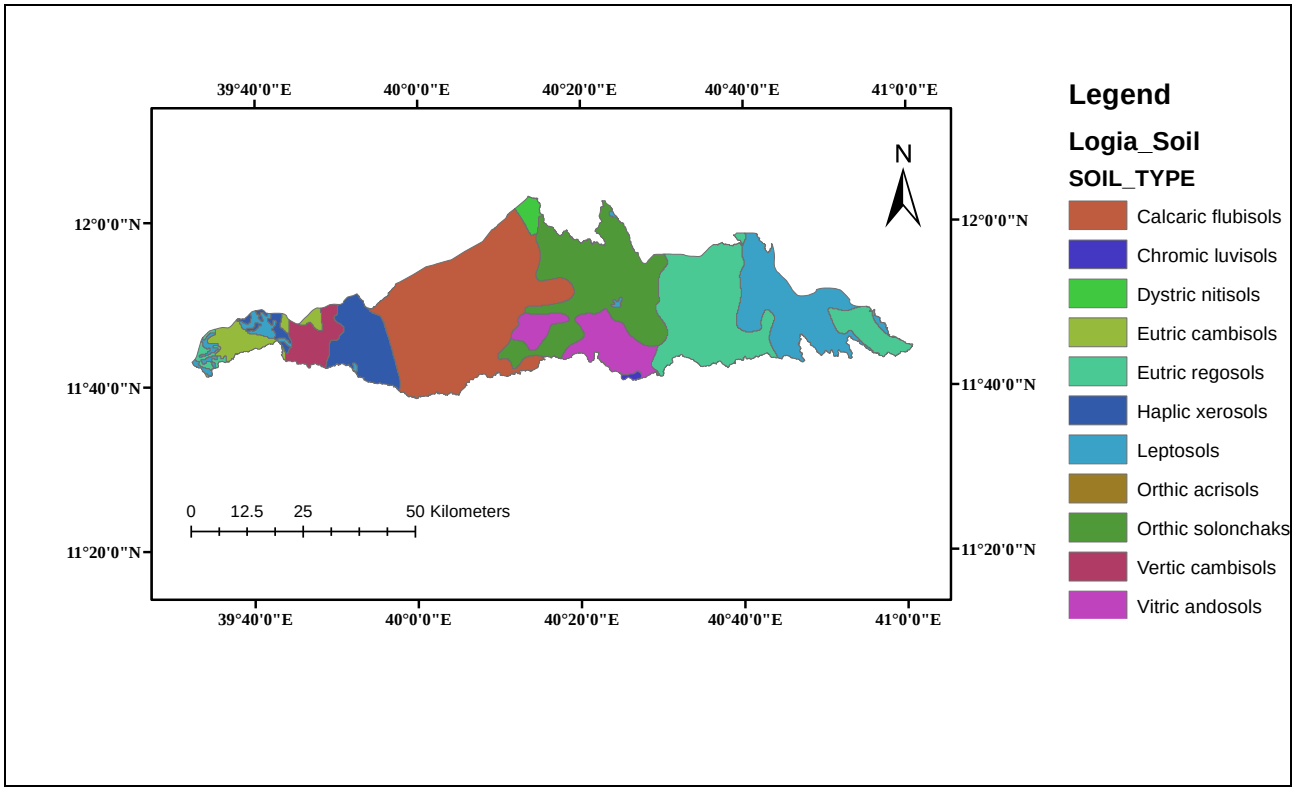

Figure 3. 4: Logia Watershed Soil Map

3.4.5 Hydraulic Modeling Using HEC-RAS

3.4.5.1 Terrain Model

One of the major problems of hydraulic modeling is that the terrain data does not often include the actual terrain underneath the water surface of the channel region. The RAS Mapper of HEC-RAS 5.0.3 version can be used to create a terrain model of the channel region from the HEC-RAS cross-section and the cross section interpolation surface (HEC, 2016). Figure 3.5 shows new terrain model created from DEM 20 m resolution. From the figure the maximum and minimum bed elevation of Logia River in the boundary of the terrain model was found 1502 m and 371 m a.m.s.l respectively.

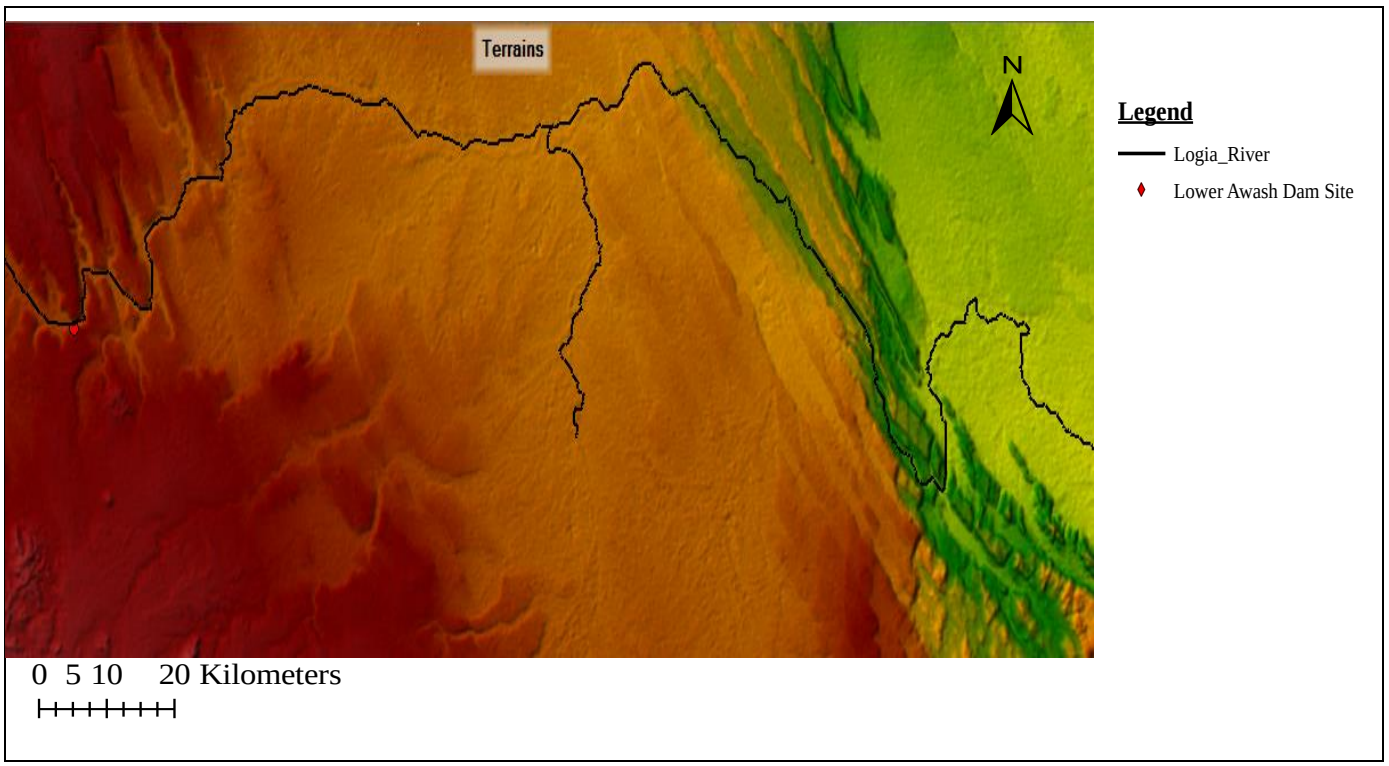

Figure 3. 5: Terrain Model of Logia River downstream of the Dam

3.4.5.2 Geometric Data on HEC-RAS

The latest version of HEC-RAS 5.0.3 now has the ability to perform two dimensional flow routing. For the dam breach study the user can model the downstream area entirely with 1D element (cross-section and storage area); as combination of 1D and 2D elements (cross-sections, storage areas and 2D flow areas); or the entire downstream area can be modeled as 2D flow area.

The 2D flow areas can be directly connected to the storage area by using a hydraulic structure called Storage Area/2D Flow Area Hydraulic Connection ("SA/2D Area connection").

In this study the storage area is to be used for representing the reservoir water. The hydraulic connection between the storage area and the 2D flow area is used to model the dam. The 2D flow area will be helpful to simulate the hydraulics of the flow downstream of the dam. The geometric data including the reservoir, the dam and the 2D flow area downstream of Lower Awash Dam area are presented on figure 3.6 below.

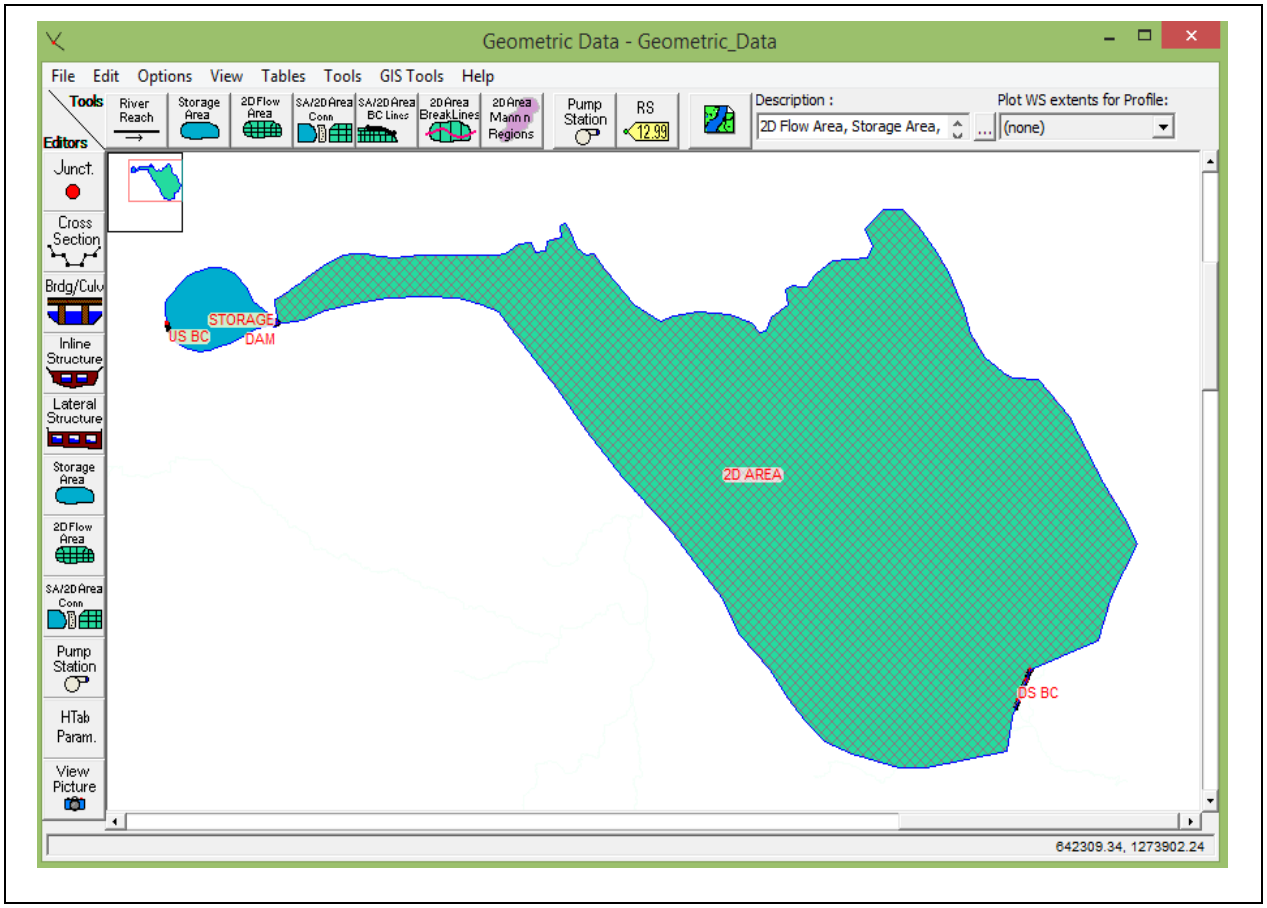

Figure 3. 6: HEC-RAS Geometric Data

Storage area/ Reservoir: Storage areas are like a region in which the water can be diverted in to or from. For this study the intended Lower Awash dam reservoir was modeled as storage area. The basic data required for storage area is elevation versus volume data obtained from the design document (see appendix A).

Storage Area/2D Area connection: Storage area /2D Area connection is used to link the storage area (reservoir) and the 2D flow area. For this study Lower Awash dam with its features was modeled as Storage area /2D Area connection. The basic information required for SA/2D Area connection includes breach plan data and embankment profile. In addition to the dam profile failure location, failure mode, full breach formation time, trigger mechanism, breach parameters data have to be filled for the SA/2D Area connection editor. Figure 3.7 shows Lower Awash dam embankment station and elevation profile.

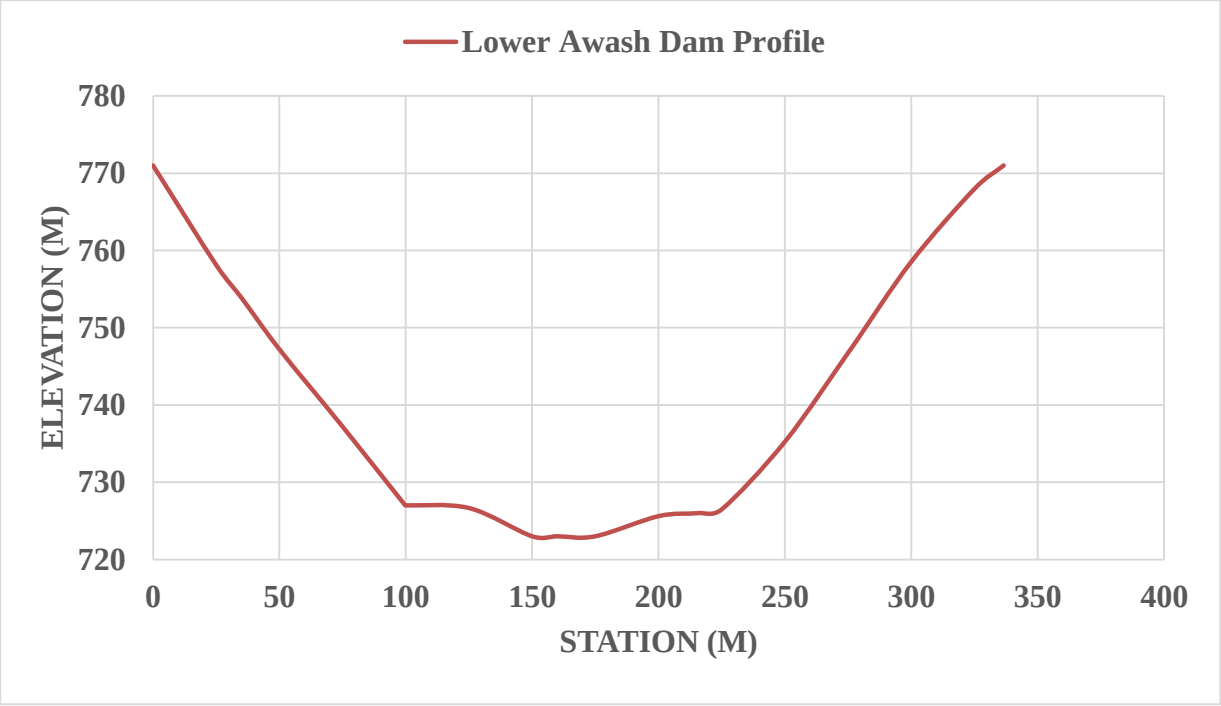

Figure 3. 7: Lower Awash Dam Embankment Profile (WWDSE, 2016)

2D Flow Area: Two dimensional flow areas (2D Flow Areas) are a region of a model in which the stage and flow through that region will be computed in HEC-RAS with two dimensional dynamic routing (discretized forms of the St. Venant Equations). A 2D flow area is defined by laying out a polygon that represents the outer boundary of 2D flow area. Then the user must define the computational mesh. For this study the area downstream of Lower Awash Dam was modeled as 2D flow area with a computational mesh size of 300m×300m as shown on the figure 3.4. The mesh contains 58,583 cells with maximum, minimum and average cell area of 191,305 m^2, 69,049 m^2, and 90,500 m^2 respectively.

3.4.5.3 Manning's Roughness Coefficient

Roughness coefficients represent the resistance to flow and flood pains. Manning's n coefficient is used in the manning equation to estimate discharge in the open channel and 2D flow area. One of the capabilities of the HEC-RAS 5.0.3 new version is that it is likely to generate spatially varying Manning's n value. This is ended by exporting the 2D flow area from the RAS Mapper as a shape file and clipped in ARC-GIS using land use land cover data of Awash sub basin.

Finally a new land cover layer is produced in the Ras mapper by adding the clipped shape file with the respected value of the Manning's n based on Chow (1959) for different land cover as shown on Figure 3.8 below. The recommended Manning's roughness Coefficients values, and land use land cover map of the 2D flow area are shown on appendix E & F respectively.

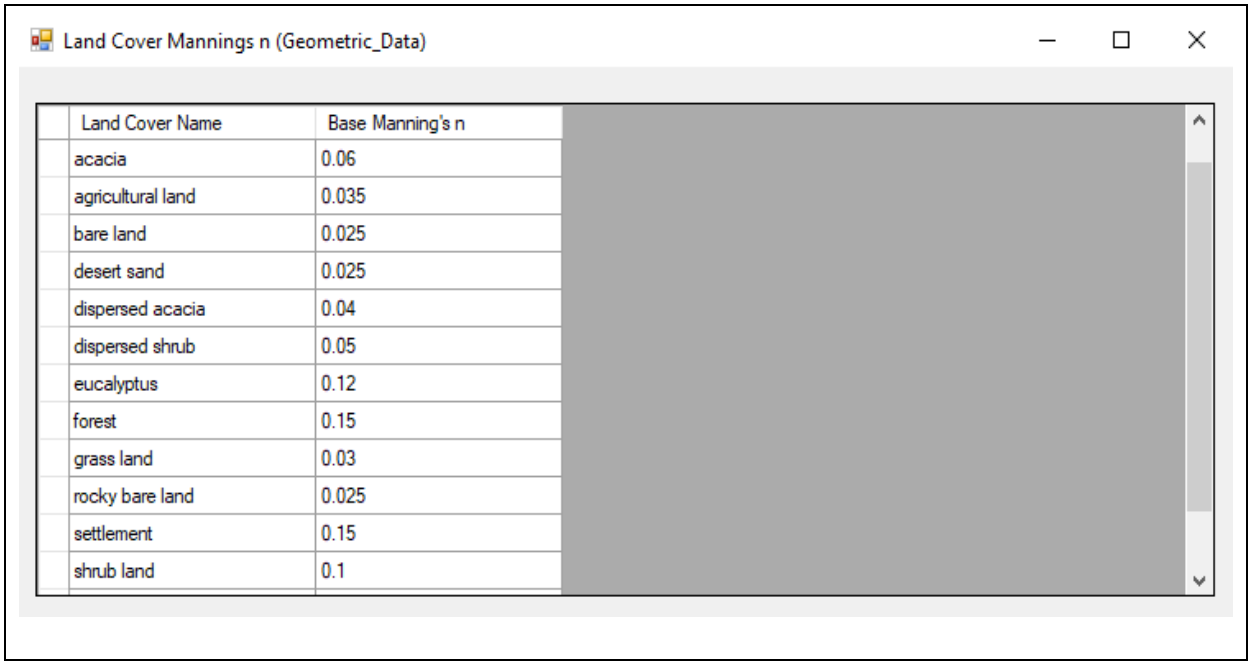

Land Cover Name	Base Manning's n
acacia	0.06
agricultural land	0.035
bare land	0.025
desert sand	0.025
dispersed acacia	0.04
dispersed shrub	0.05
eucalyptus	0.12
forest	0.15
grass land	0.03
rocky bare land	0.025
settlement	0.15
shrub land	0.1

Figure 3. 8: Manning's Roughness Coefficients Values of 2D Flow Area in RAS Mapper

3.4.5.4 Reservoir Routing (Level Pool or Dynamic)

HEC RAS can route flows in the reservoir before, during, and after the dam breach event occurred using any one of the level pool or dynamic routing (drawdown). The four independent determining variables were combined into a Compaction Factor, that measures the "Compactness" of a reservoir, and a Translation Factor, which measures the rate at which water can replenish the drawdown effect (Chris Goodell, WEST Consultants, 2015).

The compaction factor, translation factor and the drawdown number are calculated using the equations (3.9 to 3.11) below.

$$Fc = H/L \quad \text{(3.9)}$$

$$Ft = ct/L \quad \text{(3.10)}$$

Where: Fc = Reservoir Compaction Factor

Ft = Reservoir Translation Factor

H = Breach Height

t = Failure Time

c = Wave Celerity = (gD) ^0.5

L = Reservoir Length

The drawdown number, Dn, is a gage that can be used to determine when level pool reservoir Routing for dam breach events is an acceptable routing method.

$$Dn = Fc*Ft \quad \text{(3.11)}$$

The calculated drawdown number, Dn is correlated with the discharge difference, QDiffs on the curve plotted with Dn on the x-axis and QDiffs on the y-axis. High values of Dn correspond with low QDiffs, hence level pool is a good representation of reservoir drawdown. Whereas low values of Dn correspond with high QDiffs which results that level pool is not a good representation of reservoir drawdown.

3.4.5.5 Unsteady Flow Analysis

Flood is a characteristic sample of unsteady flow as the stage of the flow varies instantly as the flood tendency pass (Chow, 1960). The essential unsteady flow data should be filled to execute the unsteady flood modeling after all of the geometric data are entered inside HEC-RAS. The data required for unsteady flow analysis include upstream boundary condition, downstream boundary condition and initial condition. For this study inflow hydrograph in to the reservoir was used as upstream boundary condition, whereas downstream boundary condition is set to normal depth with a slope of 0.00001 as shown on Figure 3.9 below. The reservoir normal water level was used as initial condition. The inflow hydrograph of Logia River for the probable maximum flood, PMF is shown on appendix B.

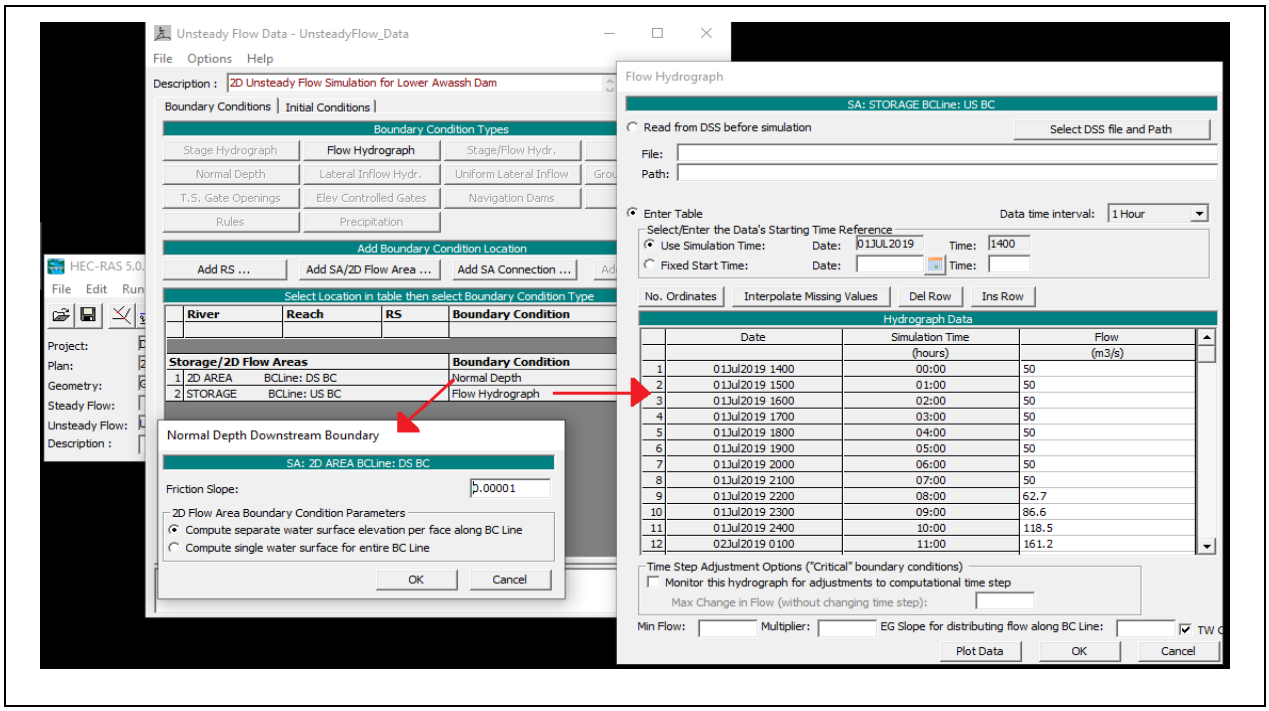

Figure 3. 9: Boundary Conditions on HEC-RAS 2D Unsteady Flow Data Editor Window

3.4.6 Dam Breach Mechanism and Breach Parameters Estimation

Since Lower Awash Dam could not be overtopped due to the PMF, the dam breach analysis will be performed only for piping mode of failure. Piping through dam body may be formed due to excessive seepage that may be triggered when the impervious core material used is poor in quality or when the construction procedure does not follow engineering standards. The proposed dam is a type of zoned rockfill having central clay core and hence the breach is modeled as an orifice flow during the initiation of the breach.

One of the capabilities of the HEC-RAS 5.03 is the possibility to calculate the breach parameters inside the software. For this study the breach parameters were calculated using HEC-RAS breach parameter calculator tab. The selected methods were Froehlich (1995a), Froehlich (2008), Macdonald and Langridge-Monopolis (1984), Von Thun and Gillette (1990), and Xu and Zhang (2009). In dam breach analysis selecting the appropriate breach parameters is very important since they have a great impact on the breach peak outflow. Once the breach parameters are calculated inside HEC-RAS breach parameter calculator tab it is important to verify the parameters using recommended range of possible values of breach parameters.

3.4.7 Breach Outflow Computation and Envelop Curves

After the analysis is completed and the hydrograph developed, it is necessary to check the reasonableness of the maximum breach outflow discharge Qmax. For this study the peak breach outflow was computed using HEC-RAS program for Froehlich (2008), and Von Thun & Gillete methods in piping failure mode. Once a breach hydrograph is computed in HEC-RAS, the computed peak flow from the model can be compared with envelope curves of historically failed dams to select the appropriate method. To do this hydraulic depth should be calculated in feet using the breach parameter information by the formula:

$$\text{Hydraulic depth (D)} = \frac{\text{Wetted area(A)}}{\text{Top width (T)}} \quad \text{.....} \quad (3.12)$$

According to HEC-RAS dam breach study (2014) training document peak envelop curve developed from historically failed dams have power trend with equation:

$$Q_B = 75D^{1.85} \quad \text{.....} \quad (3.13)$$

Where, Q_B is peak outflow in feet cubic per second and D is hydraulic depth in feet.

The difference in discharge is calculated by subtracting the peak outflow discharge Q_B from the breach peak outflow discharge computed in HEC-RAS. The method with a lower error (Q_{diff}) is taken as an appropriate method used to prepare the flood inundation maps.

3.4.8 HEC-RAS Model Calibration

For various points along the river reach on its course it is needed to calibrate the channel roughness coefficient (Manning's "n" value) through modeling of flood. The relationship of historical measured stage and discharge has been collected at Logia gaging station. In such cases, applying trial and error to modify manning roughness coefficient is very compulsory for calibration until the simulated rating curve come from HEC-RAS and the observed rating curve became close. The data during the floods for periods of 1998 as well as 1999 have been assumed for calibration of Manning's roughness coefficient "n". For justification their adequacy to the simulation of flood in Logia River reach along the channel, the values of "n" (ranging from 0.06 to 0.013) have been entered. Considering mean of optimal Manning's "n" values calculated for flood years of 1998 and also 1999 to be 0.035 for the river reach, simulation of the flood has been accomplished to year 2001 to check precision and performance of the adjusted model.

3.4.9 Flood Inundation Mapping

One of the major advantages of dam breach modeling is to map the flood affected area due to the breach out flow. After 2D unsteady flow analysis performed in HEC-RAS the flood inundation boundary, flood inundation depth, water surface elevation, and flood velocity can be observed on RAS Mapper window. For this study the flood inundation map was prepared by exporting the depth, velocity and water surface elevation as tiff file in to ARC-GIS. The trial version of ArcGoogle that is an ArcGIS extension tool was also used for visualization when the flood inundation map was prepared for piping failure modes.

3.4.10 Flood Hazard Mapping

In addition the flood hazard map should also be prepared. In this study the combined effect of depth and velocity (depth x velocity) grid was used to categorize the flood severity in to Low, Medium, High, Very High and Extreme Hazard. The flood hazard map was prepared by exporting the (depth x velocity) grid from Ras Mapper window as tiff file in to ArcGIS. ArcGoogle that is an ArcGIS extension tool was also used for visualization when the flood hazard map was prepared. The Federal Emergency Management Agency (FEMA, 2013) hazard classification was used to prepare the flood hazard map which is shown on appendix I.

CHAPTER FOUR

4. RESULT AND DISCUSSIONS

4.1 Double Mass Curve

Consistence of recorded rainfall data was checked after filling missed rainfall data. Double mass curve technique was used to test consistency of rainfall data and applied for Bati, Dubti, Mersa, Mille and Woldya stations. As observed from figure 4.1 there is no clear shift or change in slope for all stations, hence the rainfall data at all stations are consistent.

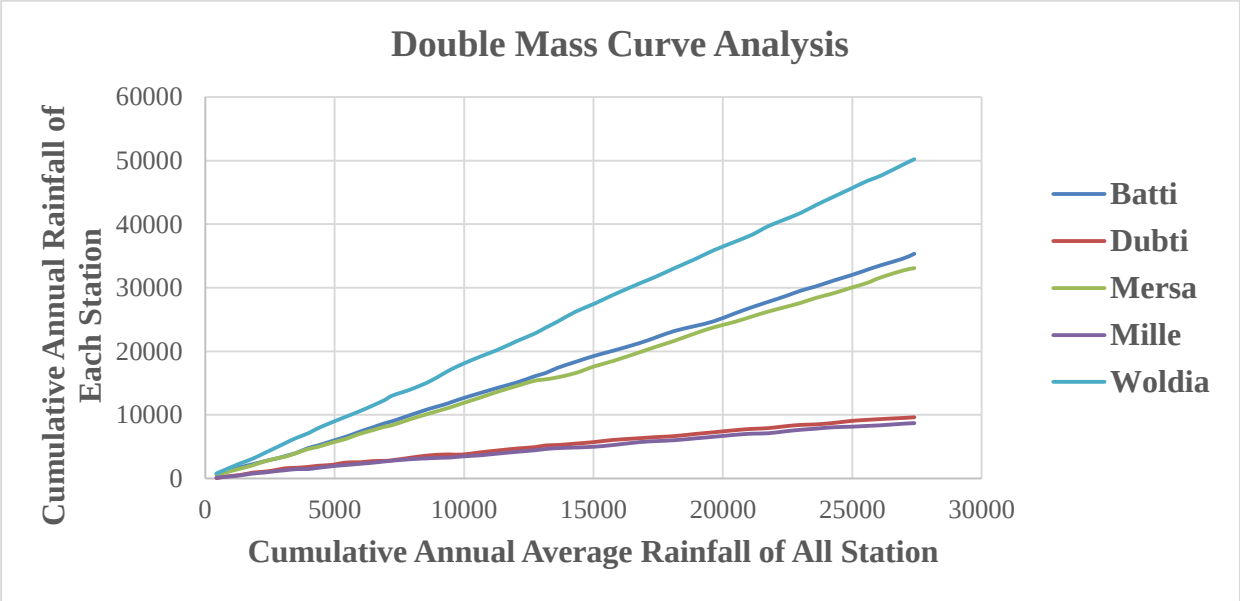

Figure 4. 1: Double mass curve of the rainfall stations

4.2 Probable Maximum Precipitation

As mentioned in the methodology part statistical technique Hershfield (1965) formula was used for estimating the probable maximum precipitation at each rainfall stations from yearly extreme daily rainfall of the rainfall stations within the study area. Therefore, 107.320 mm, 34.602 mm, 115.921 mm, 41.138 mm and 151.038 mm probable maximum precipitations were obtained from Bati, Dubti, Mersa, Mille and Woldya stations respectively. Finally the average depth of probable maximum precipitation used for the calculating the inflow hydrograph was 58.503 mm by applying 0.59 area reduction factor.

4.3 Inflow Hydrograph

In this study the inflow hydrograph of Lower Awash dam site was computed by using the standard dimensionless soil conservation service unit hydrograph method for the computed probable maximum precipitation. The probable maximum flood was also determined from the probable maximum precipitation, which was estimated based on Hirschfield's procedure. From the study the computed composite inflow hydrograph resulting from triangular hydrographs at dam site has a peak flow of 3120 m^3/s as shown on figure 4.2 below. As taken from the Lower Awash hydrological study report of WWDSE (2016), the design flood at Lower Awash dam site was selected as the 10,000 years flood and was estimated to be 1971m3/s.

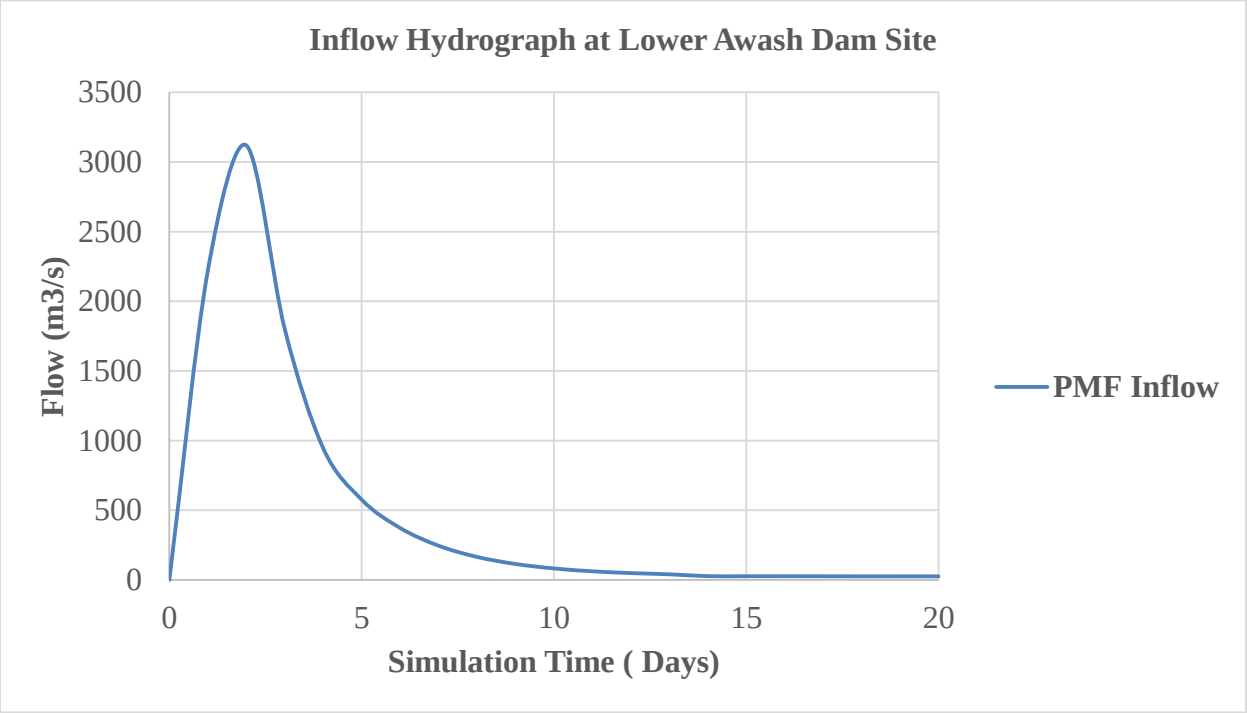

Figure 4. 2: Inflow Hydrograph at Lower Awash Dam Site

In dam breach modeling process after developing the storage area, 2D flow area, and the storage area 2D flow area connection the computed inflow hydrograph was used as an upstream boundary condition for the unsteady flow simulations in HEC-RAS. The estimated inflow hydrograph of Logia River at Lower Awash dam site that was used for the simulation purpose is clearly shown on appendix B.

4.4 Dam Breach

4.4.1 Breach Parameters

Calculating the dam breach parameters is one of the most important task that has to be done before 2D unsteady flow analysis is simulated on HEC-RAS for piping failure mode. For this study the dam breach parameters were estimated by using MacDonald and Langridge-Monopolis (1984), Froehlich (1995a, 2008), Von Thun & Gillete, and Xu & Zhang methods on HEC-RAS breach parameter calculator tab. As mentioned from the methodology part the breach shape was assumed to be trapezoidal. Table 4.1 presents summary of the results obtained from the HEC-RAS breach parameter calculator tab for piping failure mode. The breach plots are also presented below on figure 4.3.

Table 4. 1: Breach Parameters for Piping Failure Mode

Breach Parameters for Piping Failure Mode					
Method	Breach Bottom Width (m)	Right Side Slope (H:V)	Left Side Slope (H:V)	Breach Top Width (m)	Breach Formation Time (hr)
MacDonald et al	505	0.5	0.5	553	4.13
Froehlich (1995)	211	0.9	0.9	297.4	3.79
Froehlich (2008)	179	0.7	0.7	246.2	3.08
Von Thun & Gillete	146	0.5	0.5	194	1.17
Xu & Zhang	147	0.51	0.51	195.96	5.83

Once all the breach parameters are calculated it is crucial to select the suitable dimensions that actually represent the failure. From the above table 4.1 HEC-RAS breach parameter calculator for piping failure the result of breach top width calculated by MacDonald and Langridge-Monopolis (1984) was found 553m. Since the crest length of Lower Awash dam is 335m this method can be ignored for further two dimensional unsteady flow simulations, because the estimated breach top width is greater than the crest length of the dam.

The average breach width calculated from Froehlich (1995) methods was found 254.2m and this value is not acceptable for the given height of the dam (i.e. 48m) as stated in the recommendations of historical dam failures, USACE (2010). Xu & Zhang method is also ignored due to its unreliable and larger breach formation time since the method assumes the breach formation time mainly during the initiation and final completion of the erosion process. Therefore the remaining two methods will be used in the unsteady flow simulation for piping failure mode. Finally, the appropriate method for further flood inundation mapping will be selected by comparing the peak outflow floods from the two methods with the peak envelop curve. It is also observed that the breach size is related to the breach formation time. The larger the breach sizes the large the breach formation time. For comparison purpose the breach parameter can be plotted on the same chart.

From the figure it was clearly observed that the breach size for Froehlich (2008) method is larger than Von Thun & Gillete method for piping failure mode. The breach plots are scattered on spreadsheet plot as shown in the figure below. The larger the breach size will correspond to give larger peak breach outflow discharge from the simulation.

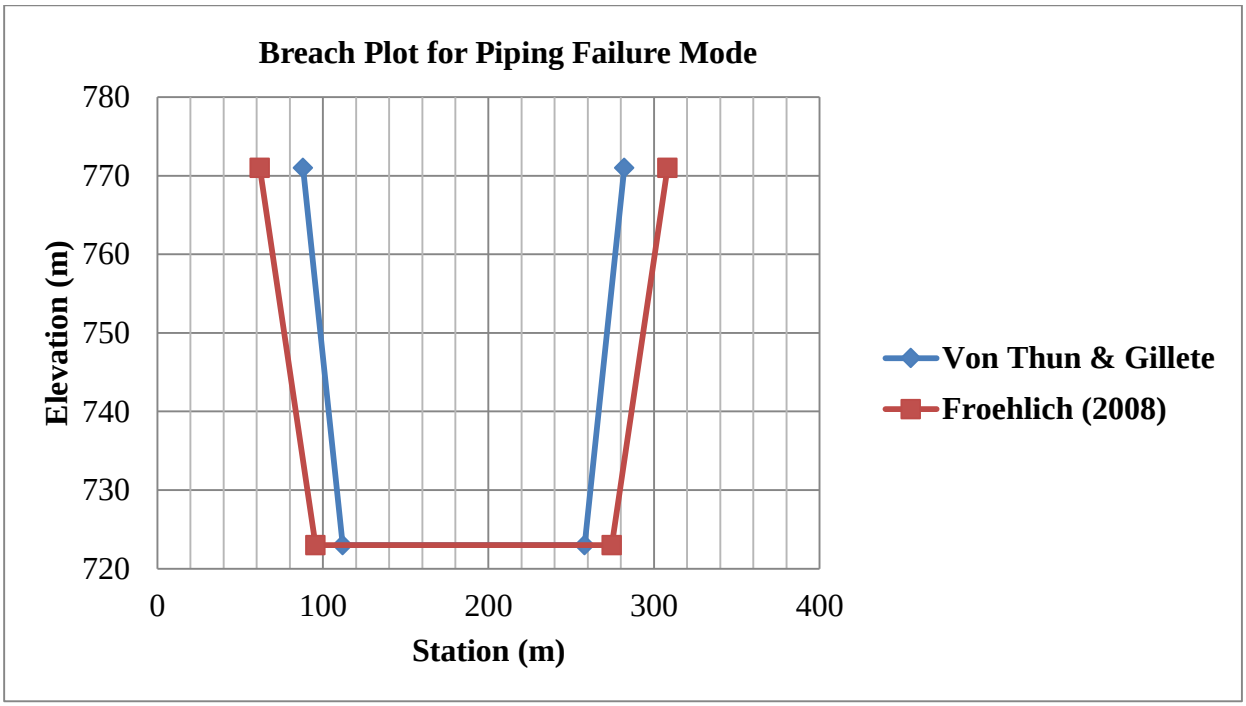

Figure 4. 3: Breach Plot Comparison for Piping Failure Mode

4.4.2 Reservoir Routing Method for Dam Breach Modeling

The reservoir compaction factor and translation factor were 0.14 and 119 respectively. Hence, the calculated drawdown number D_n was found to be 17.01. The resulting value of drawdown number D_n gives a lower value of Q_{Diffs} about 3% which is found in the lower range. Therefore level pool is an appropriate dam breach reservoir drawdown method for this study.

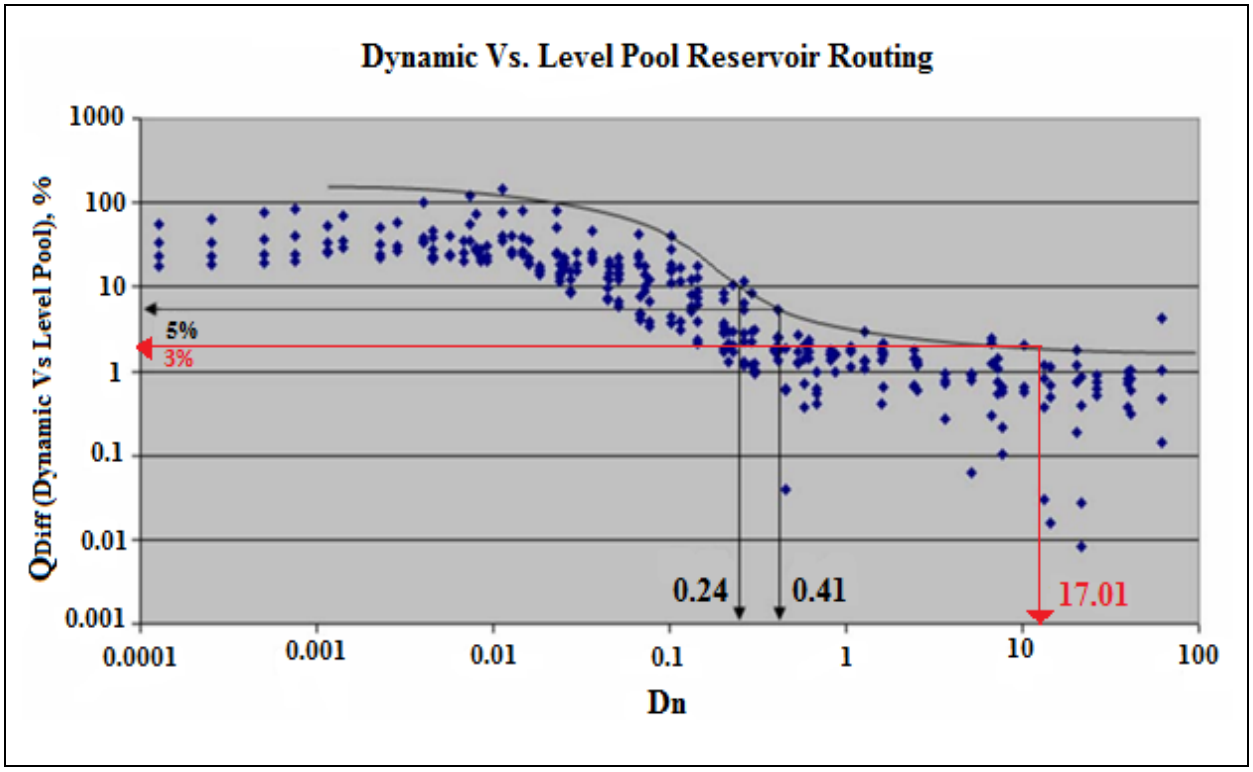

Figure 4. 4: Dynamic versus Level Pool Reservoir Routing, (WEST Consultants, 2015)

4.4.3 Breach Outflow Hydrograph

After performing 2D unsteady flow simulation for piping failure mode the peak breach outflow from Lower Awash dam on HEC-RAS was found 65,822 m^3/s and 60,072 m^3/s by Froehlich (2008) and Von Thun & Gillete methods respectively. Like breach plot compassion it is also important to compare the outflow for the two methods by plotting on the same chart. The following figure shows the breach outflow hydrograph for Froehlich (2008) and Von Thun & Gillete methods. As observed from the breach outflow hydrograph higher magnitude of peak flow was obtained on Froehlich (2008) method.

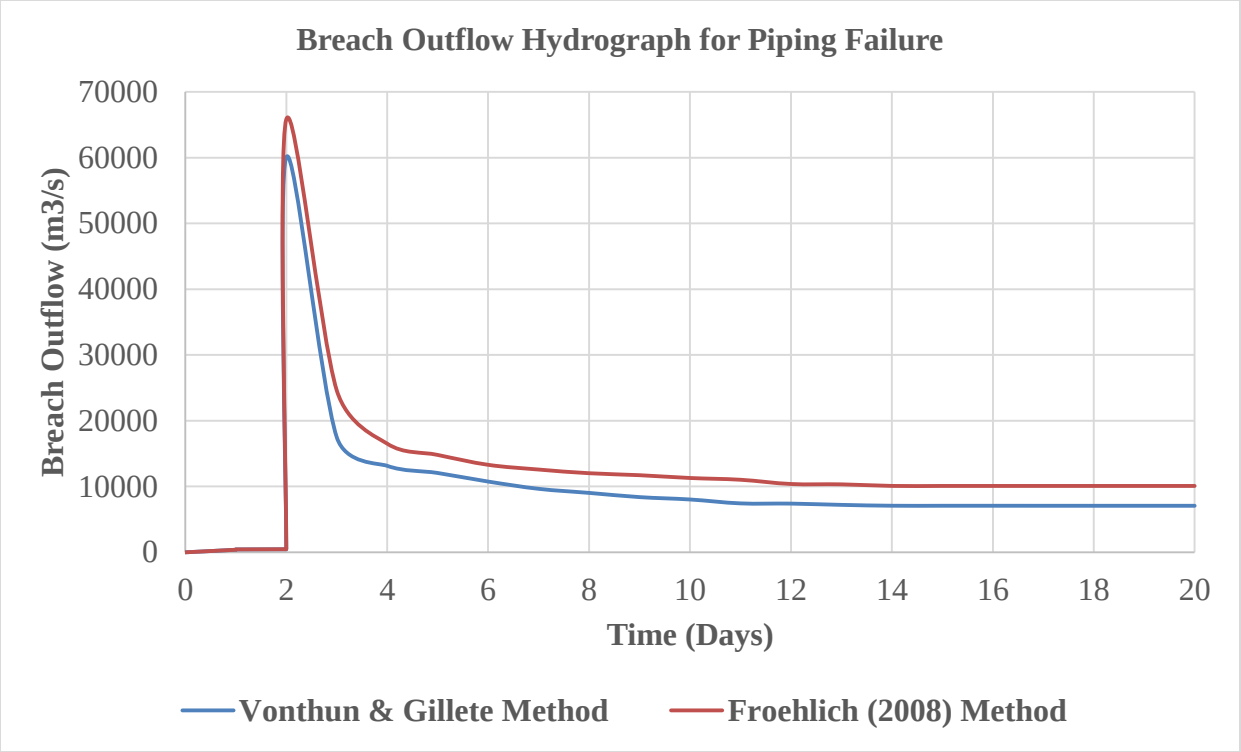

Figure 4. 5: Comparison of Breach Outflow Hydrograph for Piping Failure

4.4.4 Breach Outflow Comparison Using Historical Envelop Curves

Once a breach hydrograph is computed in HEC-RAS, the model peak outflows of the two methods were compared to envelop curve of historical failure to select the appropriate method. The hydraulic depth (D) which is the ratio of wetted area to the top width was calculated in feet. After the computation of the hydraulic depth then the peak outflow was computed as a function of hydraulic depth by using peak envelop equation. The resulting hydraulic depth and outflow was found (166.35ft, 963,725ft^3/s) and (162.42ft, 922,028ft^3/s) for Froehlich (2008) and Von Thun & Gillete methods respectively. The computed breach outflow from the HECRAS model converted to cubic feet was also 1,162,465 ft^3/s for Froehlich (2008) and 1,060,912 ft^3/s for Von Thun & Gillete method. The resulting peak outflow difference was found to be 198,739 ft^3/s and 138,884 ft^3/s for Froehlich (2008) and Von Thun & Gillete methods respectively. As presented on table 4.2 below Von Thun & Gillete method with the peak breach outflow of 1,060,912 ft^3/s has relatively the lower error and can be taken as the appropriate method used to prepare the flood inundation maps.

Table 4. 2: Breach Peak Outflow and Hydraulic Depth for Piping Failure Mode

Method	Peak outflow(m^3/s)	Peak flow(ft^3/s)	Hydraulic depth(ft)	$Q_b(ft^3/s)$	Peak flow(ft^3/s) - $Q_b(ft^{3/}s)$
Froehlich(2008)	65,822	1,162,465	166.35	963,725	198,739
Von Thun & Gillete	60,072	1,060,912	162.42	922,028	138,884

The calculated percentage discharge differences are 17.1% and 13.09 % for Froehlich (2008) method and Von Thun & Gillete method respectively. Hence, Von Thun & Gillete method with the breach outflow of 60,072 m3/s has relatively the lower discharge difference and can be taken as the appropriate method used to prepare the flood inundation maps as shown on the envelop curve developed from historically failed dams below.

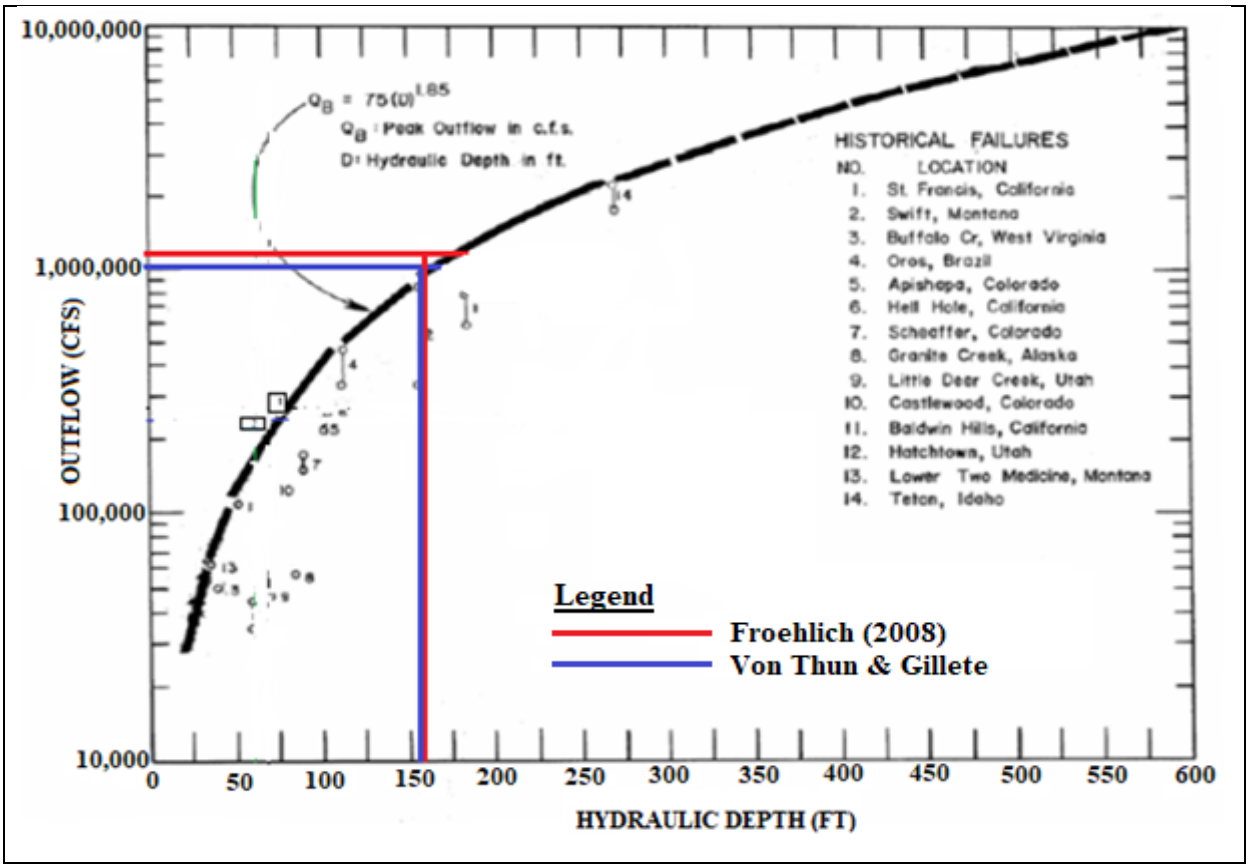

Figure 4. 6: Verification of Piping Outflows using Historical Outflow Envelope Curve

4.5 Calibration of HEC-RAS Model

Through floods simulation process the channel roughness coefficient (Manning's "n" value) was calibrated for several points in Logia River reach along the channel to excuse their suitability. Since previously counted stage and discharge relationship has been collected at Logia gaging station; trial and error technique was used to correct the manning's roughness coefficient for calibration till the simulated rating curve come from HEC-RAS and the observed rating curve has come to be alike. Having completed the calibration using different values of Manning's roughness coefficient "n" values (ranging from 0.06 to 0.013), a good closeness have been gained among model simulated and observed rating curves at Logia gauging station for the year 2001. Thus the most acceptable single value of Manning's roughness coefficient was found to be 0.035. Comparison among model simulated and practically observed and rating curves at Logia gauging station have clearly presented on Figure 4.7 below.

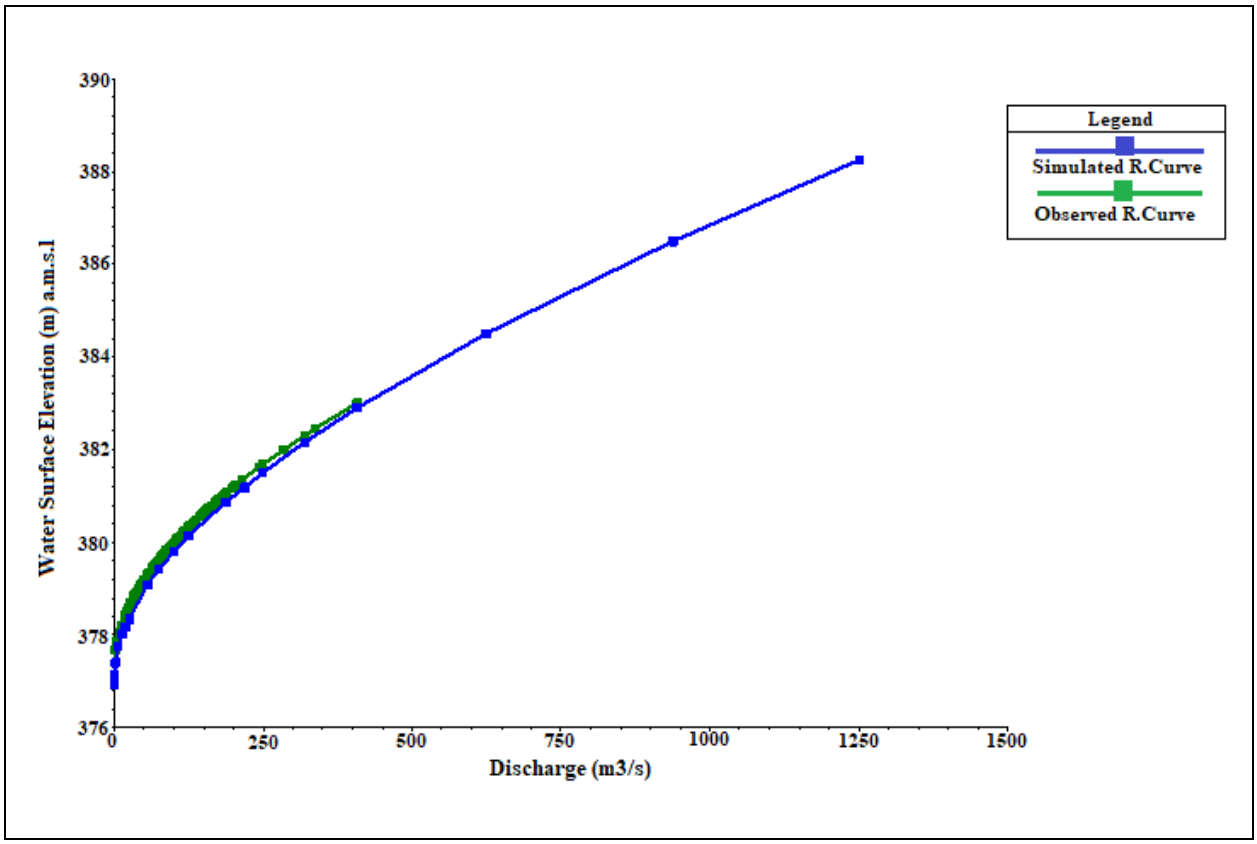

Figure 4. 7: Model Simulated Versus Observed Rating Curve at Logia Gauging Station

4.6 Flood Inundation Map

a) Flood Inundation Boundary Map

The flood inundation boundary map of the downstream prone area is presented on Figure 4.8. From the map it was obtained that the Ethio-Djbouti road between Logia and Samara towns will be flooded; the bridge at Logia will become overtopped approximately up to 5m and most probable to fail; Logia Town alongside Logia River will be affected; Dubti town will be severely flooded; Tendaho sugar factory and the irrigation infrastructures will be flooded; and a few parts of Assaita town will be affected.

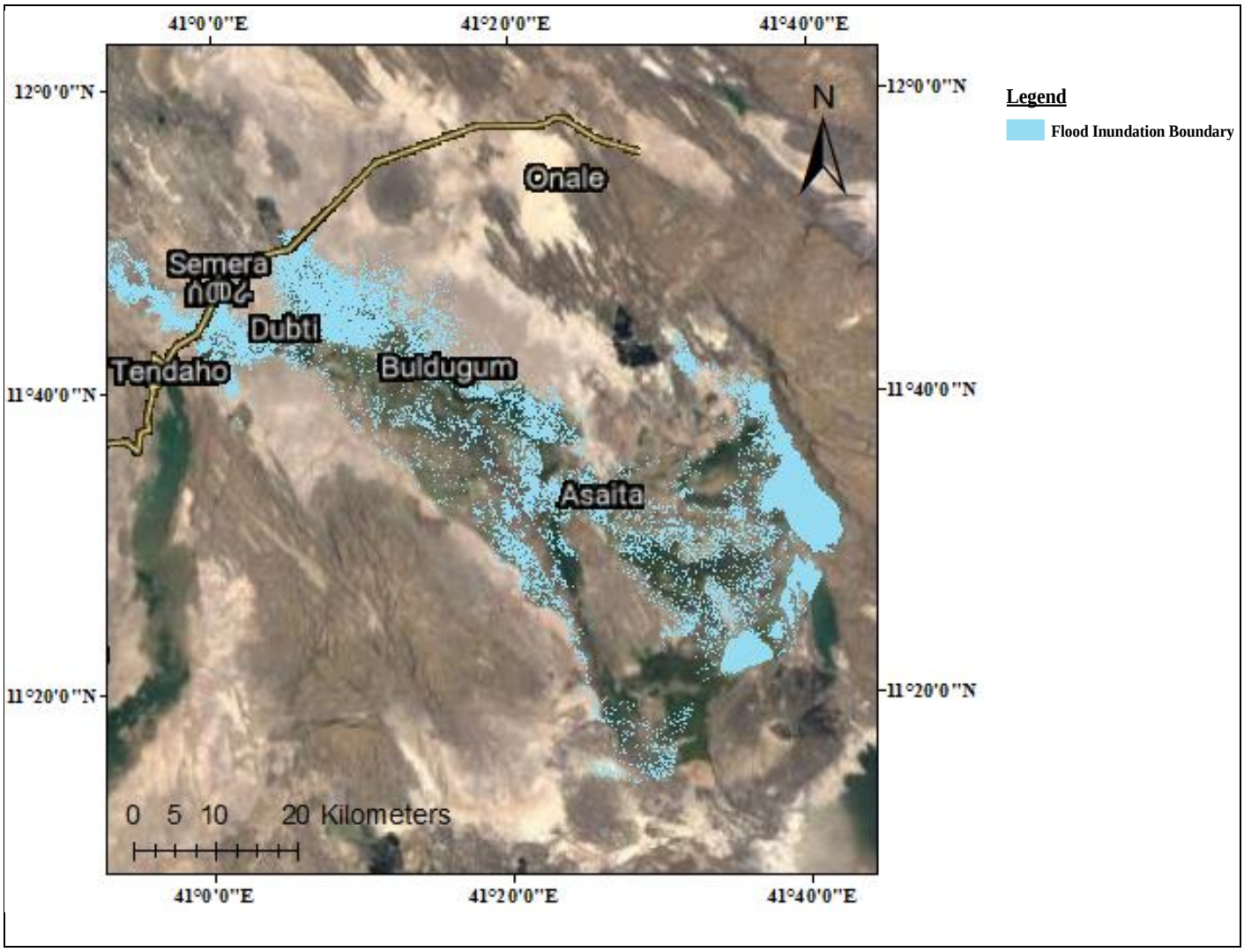

Figure 4. 8: Flood Inundation Boundary Map

b) Flood Inundation Depth Map

The flood inundation depth variation at different part of the flood plain area is presented on Figure 4.9. The minimum and the maximum inundation depths at downstream prone areas were found 0.001 and 26.1m respectively. From the figure it was observed that most of the flood plain areas are covered by a flood depth of water within the range of 0.001 to 9.5m. This flood depth can cause severe damage to the peoples and infrastructures settle downstream of the dam and near logia river flood plain.

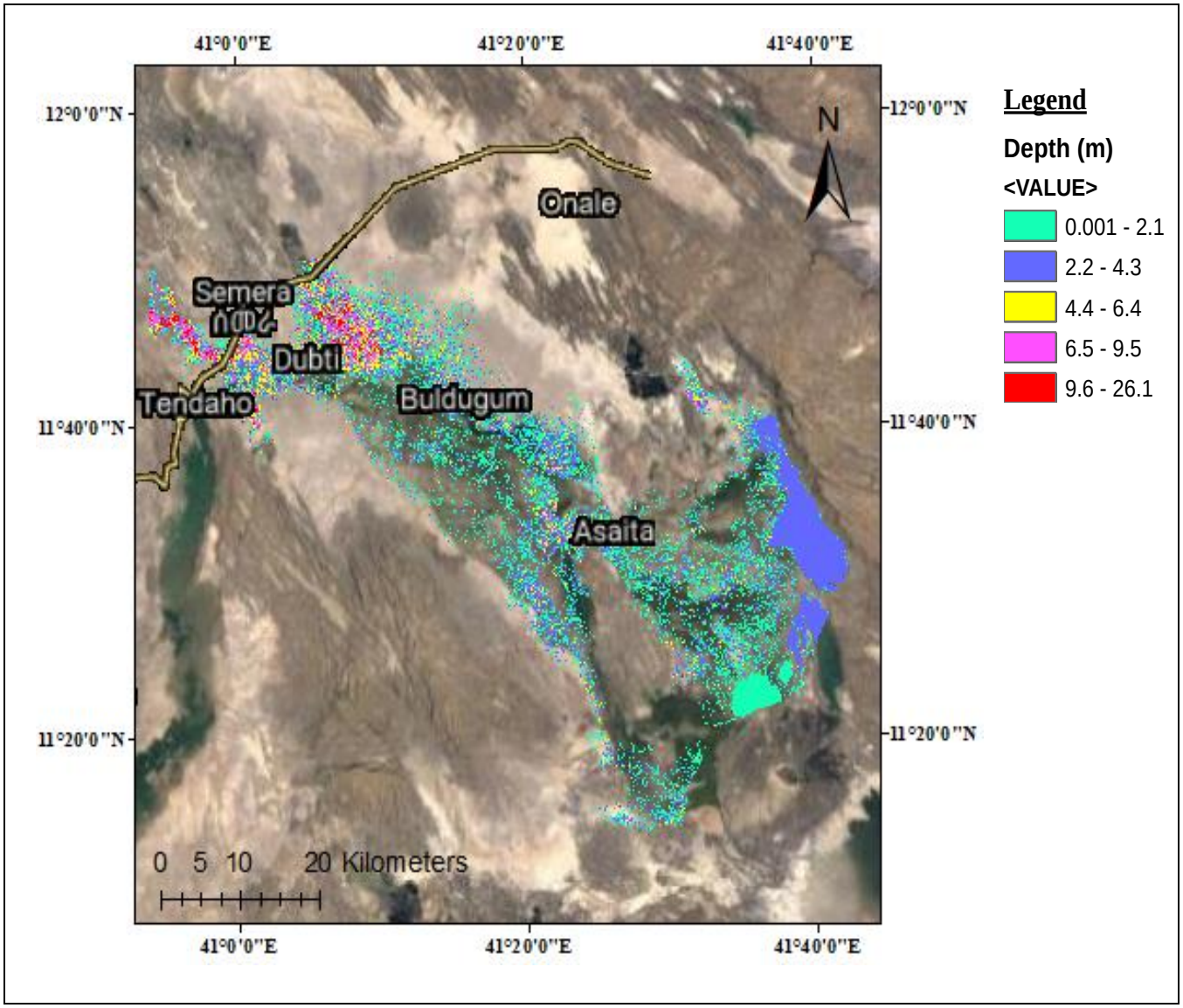

Figure 4. 9: Flood Inundation Depth Map

c) Flood Inundation Water Surface Elevation Map

In unsteady flow analysis computed water surface profile can be exported from RAS Mapper to ARC-GIS, and overlaid on ArcGoogle (Google satellite and Google Hybrid) for visualization. The various water surface elevations of the flood plain area for piping failure are presented on Figure 4.10 below. From the figure minimum and maximum water surface elevations of the flood prone areas were found 333.4 and 414.2m a.m.s.l respectively.

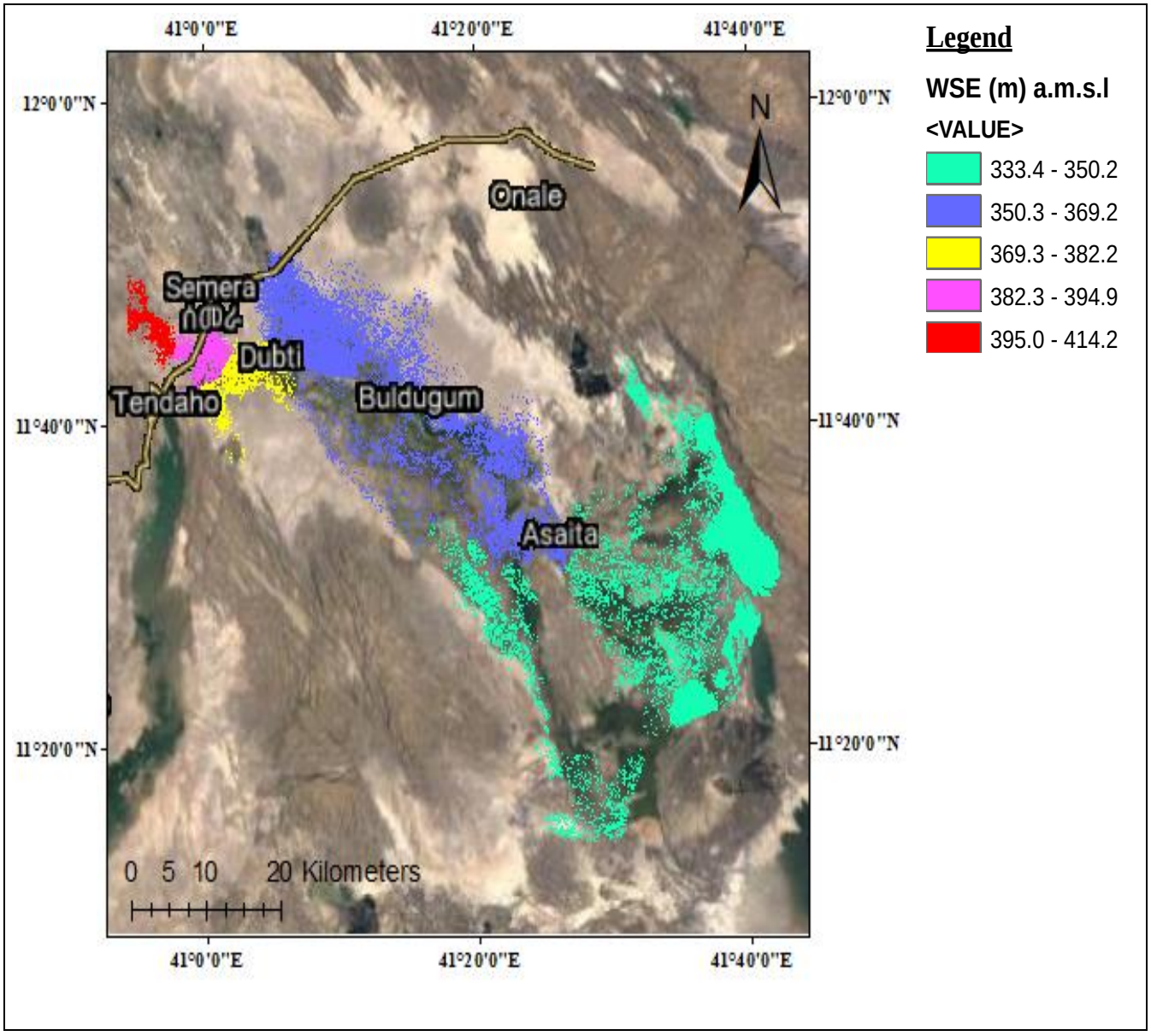

Figure 4. 10: Water Surface Elevation Map

d) Flood Inundation Velocity Map

In flood modeling velocity mapping is necessary to assess the damage caused by the flood. A flow velocity greater than 1m/s can cause structural damage of road infrastructure and residential buildings. The velocity (m/s) map of the flood plain area is presented on Figure 4.11. For this study the flood velocity ranges from 0.00001 to 4.9 m/s, and becomes zero at the final boundary of the flood plain area.

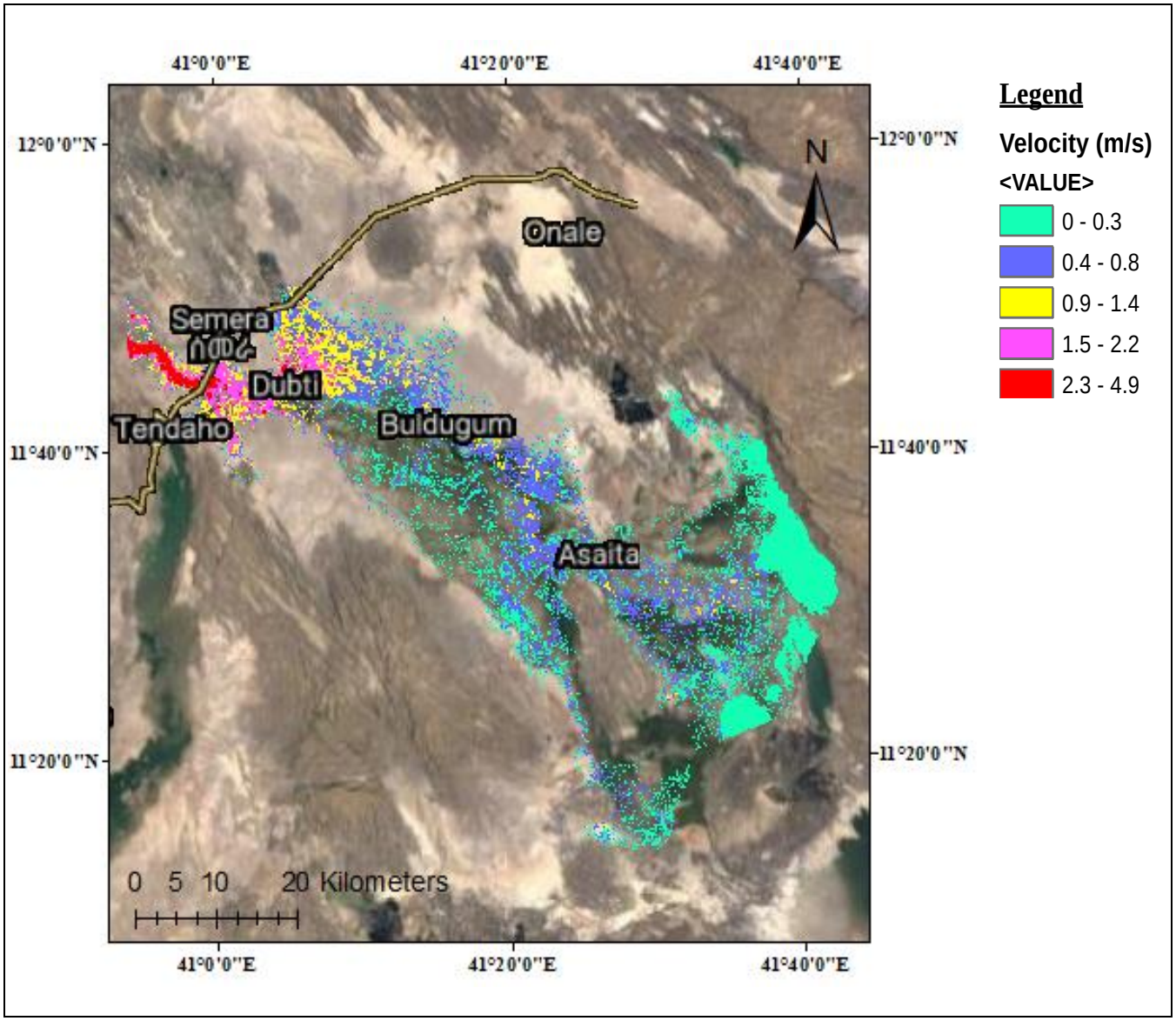

Figure 4. 11: Flood Inundation Velocity (m/s) Map

4.7 Flood Hazard Map

The combined effect of depth and velocity in the Ras Mapper was exported in to ArcGIS to prepare the flood hazard map and classify the flood hazard severity in to various categories. The trial version of ArcGoogle which is an extension tool of ArcGIS was used to visualize the hazard areas. As shown on Figure 4.12 below the flood hazard was classified from low to extreme flood hazard severities. From the map it was obtained that Assaita town, the factory and irrigation infrastructures will be susceptible to low flood hazard; Dubti town will be affected by medium to high flood hazards; Logia town near Logia river flood plain, the Ethio-Djbouti road between Logia and Samara towns, and the bridge at Logia will most probably be under extreme flood hazards due to the dam breach by piping failure.

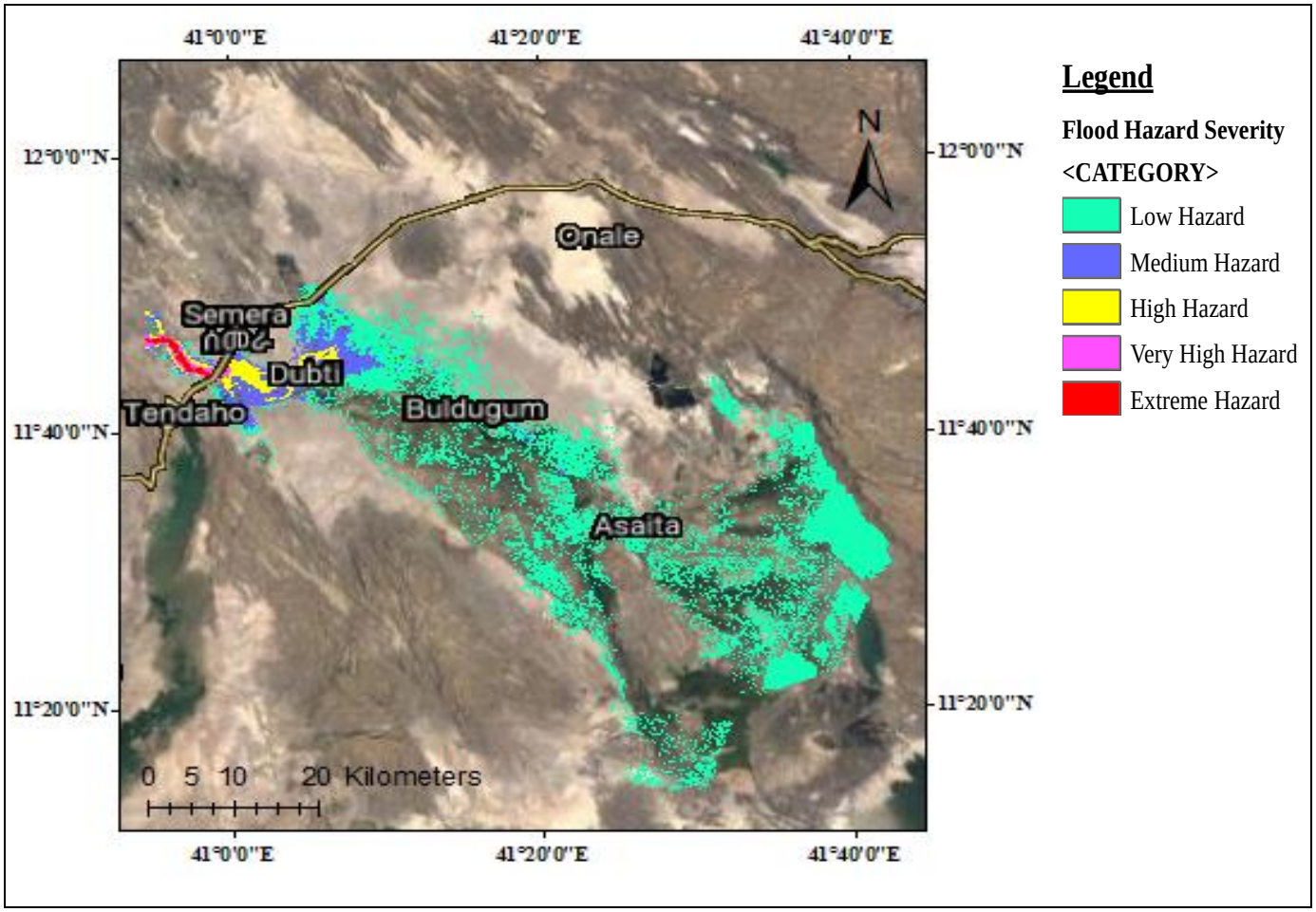

Figure 4. 12: Flood Hazard Map

CHAPTER FIVE

CONCLUSION AND RECOMMENDATION

Conclusion

The aim of this study was to analyze the dam breach events and mapping the breach outflow flood downstream of Lower Awash dam. For analysis the dam and reservoir characteristics, the inflow hydrograph, and land cover data have been used with the current recommended literatures and models. The analysis was performed for piping failure scenario using HEC-RAS two dimensional unsteady flow modeling.

The dam breach has been simulated; with a breach bottom width of 146m, and breach formation time of 1.17hr, having breach side slope 0.5. The simulated results on HEC-RAS reached peak breach outflow of 60,072 m3/s. After computation of the breach hydrograph in HEC-RAS, the model peak outflow was compared to envelop curve of historical failure for rationality. The model was calibrated by changing the Manning's "n" values to the flow years (1998-1999) and its performance was evaluated for the year 2001; reasonable agreement have been achieved between simulated and observed rating curves at Logia gauging station.

Finally the flood inundation map was prepared by exporting the flood inundation boundary, flood depth, water surface elevation and flood velocity tiff raster file from RAS Mapper to ArcGIS and overlie to ArcGoogle to visualize coverage of the flood affected area due to the breach. Moreover the flood hazard map was also prepared by exporting the combined effect of flood depth and velocity tiff raster file from RAS Mapper to ArcGIS and overlie to ArcGoogle. A maximum flood depth of 26.1m, maximum water surface elevation of 414.2m a.m.s.l., and a maximum flood velocity of 4.9 m/s were obtained from the flood inundation map. Generally as noticed from the flood inundation and flood hazard maps Logia town near Logia river flood plain, the Ethio-Djbouti road between Logia and Samara towns, and the bridge at Logia will most probably be under extreme flood hazards; Dubti town will be severely affected by medium to high flood hazards; Assaita town, Tendaho sugar factory and irrigation infrastructures will also be affected by low flood hazard due to the dam breach.

Recommendation

Since the dam breach analysis was performed to the proposed Lower Awash Dam and it is found that the dam will breach in scenario of piping failure mode. It is obvious that the dam is located in the main Ethiopia rift valley system with very high tectonic region, so effective dam monitoring and instrumentation systems should be in place to control seismic effect and further internal erosion (piping failure). High resolution DEM data of the study area should be used to increase the quality of results from two dimensional dam breach modeling. The flood mitigation potential of structural and non-structural measures that could be taken have to be planned and analyzed effectively to minimize the damage in the flood prone areas. Further study on risk assessment for the population and infrastructure that may be exposed to the flood hazard and the losses that may be incurred due to the exposure should be conducted. Finally, it is greatly recommended that the combined effect of Lower Awash and Tendaho Dams breach should be modeled since the flood prone areas downstream of both dams are the same.

REFERENCES

Abimael Leoul, (2015).Dam Breach Analysis Using HEC-RAS and HEC- GeoRAS. The Case of Kesem Kebena Dam. MSc Thesis Addis Ababa University; Ethiopia. 5p.

Adnan Arega, (2017). Dam Breach Analysis and Flood Inundation Mapping a Case Study of Koga dam. MSc Thesis Arba Minch University; Ethiopia. 3p.

Bagus Pramono Yakti, (2018). 2D Modeling of Flood Propagation due to the Failure of Way Ela Natural Dam. MATEC Web of Conferences 147, 03009 (2018).

Boussekine M., Djemili L. (2016). Modelling approach for gravity dam break analysis. Journal Of Water and Land Development.

Brunner. (2014). Using HEC-RAS for Dam Brach Studies. U.S Army corps of engineers Hydrologic Engineering Center (CEIWR-HEC) 609 second streer, Davis.

Central Water Commission (2018). Guidelines for Mapping Flood Risks Associated with Dams,

Chow, V. T., Maidment, D. R. and Mays, L. W., (1988) Applied hydrology. New York: McGraw Hill Chow, V. T., (1959), Open-Channel Hydraulics: New York, Mc Graw-Hill Book Co. 680 p. Costa,

Chris Goodell, WEST Consultants, (2015). "TD-39: Using HEC-RAS for Dam Break Studies" Hydrologic Engineering Center, Davis California.

Claudia C Hoeft & Mark Locke. (2010). Application of the inflow design flood Analysis alternative to NRCS TR-60 design storm criteria for High Hazard Dams. Washington D.C Natural Resources Conservation Service.

FEMA. (2013). Federal Guidelines for Dam Safety (Hazard Potential Classification System For Dames). United States: Homeland Security Dept., Federal Emergency Management Agency and Interagency Committee on Dam Safety.

FERC (2014) "FERC Engineering Guidelines Risk-Informed Decision Making," chapter R21, Dam Breach Analysis.

Froehlich, D. C. (1995a). Embankment dam breach parameters revisited. Water Resources Engineering, Proc. 1995 ASCE Conf. on Water Resources Engineering, New York.

Gee, D. M. (2008). Comparison of Dam Breach Parameter Estimators. Corps of Engineers Hydrologic Engineering Center. 609 2nd St., Davis, CA 95616

Habtamu Tamiru, (2019). Real Time Flood Forecasting using Artificial Neural Network (ANN) And Flood Inundation mapping. MSc Thesis Addis Ababa University, Ethiopia.1p

Hayimanot Lejissa, (2015). Dam Breach Modeling and Downstream Risk Analysis for Arjo-Dedessa Dam, MSc Thesis Addis Ababa University, Ethiopia.12p

Haile Belay, (2018). Dam Breach Analysis for Gidabo Dam, MSc Thesis Hawassa University, Ethiopia.15p

Hershfield DM. (1965). Method for estimating probable maximum precipitation. Journal American Water works Association 57: 965-972

ICOLD, (1998). Dam break Flood Analysis. Paris; International Committee on Large Dams

J Andrew Charles, B. (2011). Lessons from historical dam incidents. Bristol England: Environment Agency, Horiqon House, Eeanery Road Bristol, BS 1 5AH.

Kamal Eldin Bashar, M. K. (2005). Micro Dams. Nile Basin Capacity Building Network for River Engineering (NBCBN-RE) River Structures Research Cluster Group II.

L.H. Watkins and D. Fiddes (1984), Highway and Urban Hydrology in the Tropics, Pentech Press, Estover Road, Plymouth, Devon, UK. 85-560, Denver, Colorado.

Limin Zhang, Ming Peng, Dongsheng Chang, and Yao Xu (2016). Dam Failure Mechanisms and Risk Assessment. The Hong Kong University of Science and Technology, Hong Kong, China.

MacDonald, T. C., and Langridge-Monopolis, J. (1984) Breaching characteristics of dam failures. J. Hydraulic. Eng., 110 (5) 567–586.

Mrunal M. Joshi et al. (2017). Two dimensional dam break flow study for Ujjani dam. International Journal of Engineering and Technology (IJET).

Saqib Ehsan, Walter Marx, (2014). Dam break modeling for large earth and rockfill dams. Journal of River Engineering.

Schulze, R. E., Schmidt, E. J., and Smithers, J. C. (1992). SCS-SA User Manual PC Based SCS Design Flood Estimates for Small Catchments in Southern Africa. Pietermaritzburg: Department of Agricultural Engineering, University of Natal.

Soil Conservation Service, United States Department of Agriculture (SCS-USDA). 1986. Urban Hydrology for Small Watersheds. Washington, D. C.: U. S. Government Printing Office. Sameer SHADEED.

Tariku Tadesse, (2015).Dam Break Analysis and Risk Assessment case study of Tendaho dam. MSc Thesis Addis Ababa University, Ethiopia.

USACE, (2010) HEC-RAS, User's Manual. California: US Army Corps of Hydrological Engineering Center.

USACE, (2016) HEC-RAS, 2D Modeling User's Manual. California: US Army Corps of Hydrological Engineering Center.

Wahl, T. L. (1998). Prediction of Embankment Dam Breach Parameter. U.S. Department of the Interior Bureau of Reclamation.

Wahl, T. L. (2010). Dam Breach Modelling Analysis Methods Overview. Joint Federal Interagency Conference. Las Vegas, NV.

World Meteorological organization, (1986). Manual for Estimation of Probable maximum Precipitation. WMO No. 332.Geneva, Switzerland.

World Meteorological Organization (WMO), (1994). Guide to Hydrological Practice: Data Acquisition and Processing, Analysis, Forecasting and Other Application. 5tedition. WMO-No. 168, Geneva-Switzerland.

Wubalem Tolosa, (2018). Dam Breach Inundation Analysis for Gidabo Dam. MSc Thesis Addis Ababa University, Ethiopia, 2p.

Wurbs, R.A., 1987. Dam Breach Flood Wave Models. Journal of Hydraulic Engineering.

WWDSE. (2016). Lower Awash Multipurpose Dam and Irrigation Project Hydrology Report. Addis Ababa: Water Works Design and Supervision Enterprise.

WWDSE. (2016). Lower Awash Multipurpose Dam and Irrigation Project Final Feasibility Study & Design Report. Addis Ababa: Water Works Design and Supervision Enterprise.

Yitbarek Kifle, (2016). Dam break modelling and inundation mapping for Tendaho and Logia Dams. Addis Ababa, Ethiopia. 2p.

Zagonjolli, M. (2007). Dam Break Modelling, Risk Assessment and Uncertainty Analysis for Flood Mitigation. Delft, the Netherlands: A.A. Balkema Publisher.

APPENDIX

Appendix A: Elevation-Storage Relationship of Lower Awash Reservoir (WWDSE, 2016)

No.	ELEVATION (m.a.s.l.) (m)	Capacity (1000m3)	No.	ELEVATION (m.a.s.l.) (m)	Capacity (1000m3)
1	723.0	0	27	749.0	49101
2	724.0	5	28	750.0	55550
3	725.0	15	29	751.0	62884
4	726.0	41	30	752.0	71076
5	727.0	112	31	753.0	80278
6	728.0	276	32	754.0	90922
7	729.0	585	33	755.0	103675
8	730.0	1070	34	756.0	118848
9	731.0	1707	35	757.0	136692
10	732.0	2464	36	758.0	157783
11	733.0	3342	37	759.0	182411
12	734.0	4355	38	760.0	211041
13	735.0	5521	39	761.0	243989
14	736.0	6841	40	762.0	281280
15	737.0	8319	41	762.5	302295
16	738.0	9980	42	763.0	323309
17	739.0	11872	43	764.0	370504
18	740.0	14050	44	765.0	423133
19	741.0	16529	45	765.8	469969
20	742.0	19321	46	766.0	481677
21	743.0	22421	47	766.5	514074
22	744.0	25830	48	767.0	546471
23	745.0	29590	49	768.0	618033
24	746.0	33731	50	769.0	697118
25	747.0	38314	51	770.0	783477
26	748.0	43416	52	771.0	877131

Appendix B: PMF Inflow Hydrograph at Lower Awash Dam Site

Date	PMF Inflow (m3/s)	Date	PMF Inflow (m3/s)	Date	PMF Inflow (m3/s)	Date	PMF Inflow (m3/s)	Date	PMF Inflow (m3/s)
01Jul2019 0000	50	03Jul2019 0000	2703	05Jul2019 0000	865	07Jul2019 0000	369	09Jul2019 0000	172
01Jul2019 0100	50	03Jul2019 0100	2622	05Jul2019 0100	849	07Jul2019 0100	363	09Jul2019 0100	170
01Jul2019 0200	50	03Jul2019 0200	2543	05Jul2019 0200	833	07Jul2019 0200	357	09Jul2019 0200	167
01Jul2019 0300	50	03Jul2019 0300	2465	05Jul2019 0300	818	07Jul2019 0300	351	09Jul2019 0300	165
01Jul2019 0400	50	03Jul2019 0400	2389	05Jul2019 0400	803	07Jul2019 0400	345	09Jul2019 0400	162
01Jul2019 0500	50	03Jul2019 0500	2313	05Jul2019 0500	788	07Jul2019 0500	339	09Jul2019 0500	160
01Jul2019 0600	50	03Jul2019 0600	2239	05Jul2019 0600	774	07Jul2019 0600	333	09Jul2019 0600	158
01Jul2019 0700	50	03Jul2019 0700	2164	05Jul2019 0700	760	07Jul2019 0700	328	09Jul2019 0700	156
01Jul2019 0800	63	03Jul2019 0800	2093	05Jul2019 0800	746	07Jul2019 0800	322	09Jul2019 0800	154
01Jul2019 0900	87	03Jul2019 0900	2025	05Jul2019 0900	733	07Jul2019 0900	317	09Jul2019 0900	151
01Jul2019 1000	119	03Jul2019 1000	1969	05Jul2019 1000	720	07Jul2019 1000	312	09Jul2019 1000	149
01Jul2019 1100	161	03Jul2019 1100	1917	05Jul2019 1100	707	07Jul2019 1100	307	09Jul2019 1100	147
01Jul2019 1200	232	03Jul2019 1200	1870	05Jul2019 1200	694	07Jul2019 1200	302	09Jul2019 1200	145
01Jul2019 1300	361	03Jul2019 1300	1824	05Jul2019 1300	682	07Jul2019 1300	297	09Jul2019 1300	143
01Jul2019 1400	534	03Jul2019 1400	1781	05Jul2019 1400	670	07Jul2019 1400	292	09Jul2019 1400	141
01Jul2019 1500	734	03Jul2019 1500	1739	05Jul2019 1500	658	07Jul2019 1500	287	09Jul2019 1500	139
01Jul2019 1600	945	03Jul2019 1600	1698	05Jul2019 1600	646	07Jul2019 1600	283	09Jul2019 1600	138
01Jul2019 1700	1187	03Jul2019 1700	1659	05Jul2019 1700	634	07Jul2019 1700	278	09Jul2019 1700	136
01Jul2019 1800	1513	03Jul2019 1800	1622	05Jul2019 1800	623	07Jul2019 1800	273	09Jul2019 1800	134
01Jul2019 1900	2074	03Jul2019 1900	1585	05Jul2019 1900	612	07Jul2019 1900	269	09Jul2019 1900	132
01Jul2019 2000	2791	03Jul2019 2000	1550	05Jul2019 2000	601	07Jul2019 2000	265	09Jul2019 2000	130
01Jul2019 2100	3434	03Jul2019 2100	1516	05Jul2019 2100	591	07Jul2019 2100	260	09Jul2019 2100	129
01Jul2019 2200	3909	03Jul2019 2200	1483	05Jul2019 2200	580	07Jul2019 2200	256	09Jul2019 2200	127
01Jul2019 2300	4228	03Jul2019 2300	1450	05Jul2019 2300	570	07Jul2019 2300	252	09Jul2019 2300	125
02Jul2019 0000	4436	04Jul2019 0000	1419	06Jul2019 0000	560	08Jul2019 0000	248	10Jul2019 0000	124
02Jul2019 0100	4567	04Jul2019 0100	1389	06Jul2019 0100	550	08Jul2019 0100	244	10Jul2019 0100	122
02Jul2019 0200	4644	04Jul2019 0200	1359	06Jul2019 0200	541	08Jul2019 0200	241	10Jul2019 0200	121
02Jul2019 0300	4680	04Jul2019 0300	1331	06Jul2019 0300	531	08Jul2019 0300	237	10Jul2019 0300	119
02Jul2019 0400	4680	04Jul2019 0400	1303	06Jul2019 0400	522	08Jul2019 0400	233	10Jul2019 0400	118
02Jul2019 0500	4644	04Jul2019 0500	1276	06Jul2019 0500	513	08Jul2019 0500	229	10Jul2019 0500	116
02Jul2019 0600	4570	04Jul2019 0600	1251	06Jul2019 0600	504	08Jul2019 0600	226	10Jul2019 0600	115
02Jul2019 0700	4469	04Jul2019 0700	1225	06Jul2019 0700	495	08Jul2019 0700	222	10Jul2019 0700	114
02Jul2019 0800	4358	04Jul2019 0800	1200	06Jul2019 0800	486	08Jul2019 0800	219	10Jul2019 0800	112
02Jul2019 0900	4241	04Jul2019 0900	1175	06Jul2019 0900	478	08Jul2019 0900	216	10Jul2019 0900	111
02Jul2019 1000	4122	04Jul2019 1000	1150	06Jul2019 1000	470	08Jul2019 1000	212	10Jul2019 1000	109
02Jul2019 1100	4001	04Jul2019 1100	1126	06Jul2019 1100	461	08Jul2019 1100	209	10Jul2019 1100	108
02Jul2019 1200	3881	04Jul2019 1200	1102	06Jul2019 1200	454	08Jul2019 1200	206	10Jul2019 1200	107
02Jul2019 1300	3763	04Jul2019 1300	1078	06Jul2019 1300	446	08Jul2019 1300	203	10Jul2019 1300	106
02Jul2019 1400	3647	04Jul2019 1400	1055	06Jul2019 1400	438	08Jul2019 1400	200	10Jul2019 1400	104
02Jul2019 1500	3534	04Jul2019 1500	1033	06Jul2019 1500	431	08Jul2019 1500	197	10Jul2019 1500	103
02Jul2019 1600	3424	04Jul2019 1600	1012	06Jul2019 1600	423	08Jul2019 1600	194	10Jul2019 1600	102
02Jul2019 1700	3318	04Jul2019 1700	991	06Jul2019 1700	416	08Jul2019 1700	191	10Jul2019 1700	101
02Jul2019 1800	3217	04Jul2019 1800	971	06Jul2019 1800	409	08Jul2019 1800	188	10Jul2019 1800	100
02Jul2019 1900	3121	04Jul2019 1900	952	06Jul2019 1900	402	08Jul2019 1900	185	10Jul2019 1900	99
02Jul2019 2000	3031	04Jul2019 2000	934	06Jul2019 2000	395	08Jul2019 2000	182	10Jul2019 2000	98
02Jul2019 2100	2946	04Jul2019 2100	916	06Jul2019 2100	388	08Jul2019 2100	180	10Jul2019 2100	96
02Jul2019 2200	2866	04Jul2019 2200	898	06Jul2019 2200	382	08Jul2019 2200	177	10Jul2019 2200	95
02Jul2019 2300	2785	04Jul2019 2300	881	06Jul2019 2300	375	08Jul2019 2300	175	10Jul2019 2300	94

Date	PMF Inflow (m3/s)	Date	PMF Inflow (m3/s)	Date	PMF Inflow (m3/s)	Date	PMF Inflow (m3/s)	Date	PMF Inflow (m3/s)
11Jul2019 0000	93	13Jul2019 0000	61	15Jul2019 0000	50	17Jul2019 0000	50	19Jul2019 0000	50
11Jul2019 0100	92	13Jul2019 0100	60	15Jul2019 0100	50	17Jul2019 0100	50	19Jul2019 0100	50
11Jul2019 0200	91	13Jul2019 0200	60	15Jul2019 0200	50	17Jul2019 0200	50	19Jul2019 0200	50
11Jul2019 0300	90	13Jul2019 0300	59	15Jul2019 0300	50	17Jul2019 0300	50	19Jul2019 0300	50
11Jul2019 0400	90	13Jul2019 0400	58	15Jul2019 0400	50	17Jul2019 0400	50	19Jul2019 0400	50
11Jul2019 0500	89	13Jul2019 0500	58	15Jul2019 0500	50	17Jul2019 0500	50	19Jul2019 0500	50
11Jul2019 0600	88	13Jul2019 0600	57	15Jul2019 0600	50	17Jul2019 0600	50	19Jul2019 0600	50
11Jul2019 0700	87	13Jul2019 0700	56	15Jul2019 0700	50	17Jul2019 0700	50	19Jul2019 0700	50
11Jul2019 0800	86	13Jul2019 0800	55	15Jul2019 0800	50	17Jul2019 0800	50	19Jul2019 0800	50
11Jul2019 0900	85	13Jul2019 0900	50	15Jul2019 0900	50	17Jul2019 0900	50	19Jul2019 0900	50
11Jul2019 1000	84	13Jul2019 1000	50	15Jul2019 1000	50	17Jul2019 1000	50	19Jul2019 1000	50
11Jul2019 1100	83	13Jul2019 1100	50	15Jul2019 1100	50	17Jul2019 1100	50	19Jul2019 1100	50
11Jul2019 1200	83	13Jul2019 1200	50	15Jul2019 1200	50	17Jul2019 1200	50	19Jul2019 1200	50
11Jul2019 1300	82	13Jul2019 1300	50	15Jul2019 1300	50	17Jul2019 1300	50	19Jul2019 1300	50
11Jul2019 1400	81	13Jul2019 1400	50	15Jul2019 1400	50	17Jul2019 1400	50	19Jul2019 1400	50
11Jul2019 1500	80	13Jul2019 1500	50	15Jul2019 1500	50	17Jul2019 1500	50	19Jul2019 1500	50
11Jul2019 1600	80	13Jul2019 1600	50	15Jul2019 1600	50	17Jul2019 1600	50	19Jul2019 1600	50
11Jul2019 1700	79	13Jul2019 1700	50	15Jul2019 1700	50	17Jul2019 1700	50	19Jul2019 1700	50
11Jul2019 1800	78	13Jul2019 1800	50	15Jul2019 1800	50	17Jul2019 1800	50	19Jul2019 1800	50
11Jul2019 1900	77	13Jul2019 1900	50	15Jul2019 1900	50	17Jul2019 1900	50	19Jul2019 1900	50
11Jul2019 2000	77	13Jul2019 2000	50	15Jul2019 2000	50	17Jul2019 2000	50	19Jul2019 2000	50
11Jul2019 2100	76	13Jul2019 2100	50	15Jul2019 2100	50	17Jul2019 2100	50	19Jul2019 2100	50
11Jul2019 2200	75	13Jul2019 2200	50	15Jul2019 2200	50	17Jul2019 2200	50	19Jul2019 2200	50
11Jul2019 2300	75	13Jul2019 2300	50	15Jul2019 2300	50	17Jul2019 2300	50	19Jul2019 2300	50
12Jul2019 0000	74	14Jul2019 0000	50	16Jul2019 0000	50	18Jul2019 0000	50	20Jul2019 0000	50
12Jul2019 0100	73	14Jul2019 0100	50	16Jul2019 0100	50	18Jul2019 0100	50		
12Jul2019 0200	73	14Jul2019 0200	50	16Jul2019 0200	50	18Jul2019 0200	50		
12Jul2019 0300	72	14Jul2019 0300	50	16Jul2019 0300	50	18Jul2019 0300	50		
12Jul2019 0400	72	14Jul2019 0400	50	16Jul2019 0400	50	18Jul2019 0400	50		
12Jul2019 0500	71	14Jul2019 0500	50	16Jul2019 0500	50	18Jul2019 0500	50		
12Jul2019 0600	70	14Jul2019 0600	50	16Jul2019 0600	50	18Jul2019 0600	50		
12Jul2019 0700	70	14Jul2019 0700	50	16Jul2019 0700	50	18Jul2019 0700	50		
12Jul2019 0800	69	14Jul2019 0800	50	16Jul2019 0800	50	18Jul2019 0800	50		
12Jul2019 0900	69	14Jul2019 0900	50	16Jul2019 0900	50	18Jul2019 0900	50		
12Jul2019 1000	68	14Jul2019 1000	50	16Jul2019 1000	50	18Jul2019 1000	50		
12Jul2019 1100	68	14Jul2019 1100	50	16Jul2019 1100	50	18Jul2019 1100	50		
12Jul2019 1200	67	14Jul2019 1200	50	16Jul2019 1200	50	18Jul2019 1200	50		
12Jul2019 1300	67	14Jul2019 1300	50	16Jul2019 1300	50	18Jul2019 1300	50		
12Jul2019 1400	66	14Jul2019 1400	50	16Jul2019 1400	50	18Jul2019 1400	50		
12Jul2019 1500	66	14Jul2019 1500	50	16Jul2019 1500	50	18Jul2019 1500	50		
12Jul2019 1600	65	14Jul2019 1600	50	16Jul2019 1600	50	18Jul2019 1600	50		
12Jul2019 1700	65	14Jul2019 1700	50	16Jul2019 1700	50	18Jul2019 1700	50		
12Jul2019 1800	64	14Jul2019 1800	50	16Jul2019 1800	50	18Jul2019 1800	50		
12Jul2019 1900	64	14Jul2019 1900	50	16Jul2019 1900	50	18Jul2019 1900	50		
12Jul2019 2000	63	14Jul2019 2000	50	16Jul2019 2000	50	18Jul2019 2000	50		
12Jul2019 2100	63	14Jul2019 2100	50	16Jul2019 2100	50	18Jul2019 2100	50		
12Jul2019 2200	62	14Jul2019 2200	50	16Jul2019 2200	50	18Jul2019 2200	50		
12Jul2019 2300	62	14Jul2019 2300	50	16Jul2019 2300	50	18Jul2019 2300	50		

Appendix C: Lower Awash Dam Station and Elevation (WWDSE, 2016)

No.	Station (m)	Elevation (m)	No.	Station (m)	Elevation (m)
1	0	771	11	175	723
2	25	758.11	12	200	725.61
3	35	753.87	13	215.65	726
4	50	747.20	14	225	726.49
5	75	737.20	15	250	735.25
6	99.56	727.09	16	275	746.75
7	100	727	17	278.22	748.25
8	125	726.659	18	300	758.54
9	150	723	19	325	767.98
10	160	723	20	336.54	771

Appendix D: Ranges of Possible Values for Breach Characteristic (Gee, 2008)

Dam Type	**Average Breach Width, B_{av}**	**Horizontal component of Breach Side Slope (H), H:1V**	**Failure Time, tr (hrs)**	**Agency**
Earthern/ Rockfill	(0.5 to 3.0) × HD	0 to 1.0	0.5 to 4.0	USACE (1980)
	(0.5 to 5.0) × HD	0 to 1.0	0.1 to 4.0*	USACE (2007)
	(1.0 to 5.0) × HD	0 to 1.0	0.1 to 1.0	FERC (1988)
	(2.0 to 5.0) × HD	0 to 1.0 (slightly larger)	0.1 to 1.0	NWS (Fread, 2006)
Concrete Gravity	Multiple Monoliths	Vertical	0.1 to 0.5	USACE (2007)
	Usually ≤ 0.5L	Vertical	0.1 to 0.3	FERC
	Usually ≤ 0.5L	Vertical	0.1 to 0.2	NWS
Concrete Arch	Entire Dam	Valley wall slope	≤ 0.1	USACE (1980)
	(0.8 × L) to L	0 to valley walls	≤ 0.1	USACE (2007)
	Entire Dam	0 to valley walls	≤ 0.1	FERC
	(0.8 × L) to L	0 to valley walls	≤ 0.1	NWS
Slag/ Refuse	(0.8 × L) to L	1.0 to 2.0	0.1 to 0.3	FERC
	(0.8 × L) to L		≤ 0.1	NWS

Where: H_D = Dam Height
L = Crest Length of dam

Appendix E: Manning's n Values for Numerous Land Covers (Curtis Janssen, SCE, 2016)

Towards practice for Dam Breach Analyses study by the NRCS in Kansa, (2011 National Land Cover Data Set (NLCD), Open-Channel Hydraulics, by Chow, Ven Te, 1959, and HEC-RAS River Analysis System 2D Modeling User's Manual, Version 5.0, February 2016, Figure 3-19).

Normal Manning's n Value	Allowable Range of n Value	Land Cover Type	Land Cover Definition
0.040	0.025--0.05	Open Water	All areas of open water, generally with less than 25% cover or vegetation or soil
0.040	0.03--0.05	Developed, Open Space	Includes areas with a mixture of some constructed materials, but mostly vegetation in the form of lawn grasses. Impervious surfaces account for less than 20 percent of total cover. These areas most commonly include large-lot single-family housing units, parks, golf courses, and vegetation planted in developed settings for recreation, erosion control, or aesthetic purposes.
0.100	0.08--0.12	Developed, Low Intensity	Includes areas with a mixture of constructed materials and vegetation. Impervious surfaces account for 20-49 percent of total cover. These areas most commonly include single-family housing units.
0.080	0.06--0.14	Developed, Medium Intensity	Includes areas with a mixture of constructed materials and vegetation. Impervious surfaces account for 50-79 percent of the total cover. These areas most commonly include single-family housing units.
0.150	0.12-0.20	Developed, High Intensity	Includes highly developed areas where people reside or work in high numbers. Examples include apartment complexes, row houses and commercial/industrial. Impervious surfaces account for 80 to 100 percent of the total cover.
0.025	0.023--0.03	Barren Land (Rock/Sand/Clay)	Barren areas of bedrock, desert pavement, scarps, talus, slides, volcanic material, glacial debris, sand dunes, strip mines, gravel pits and other accumulations of earthen material. Generally, vegetation accounts for less than 15% of total cover.
0.160	0.10--0.16	Deciduous Forest	Areas dominated by trees generally greater than 5 meters tall, and greater than 20% of total vegetation cover. More than 75 percent of the tree species shed foliage simultaneously in response to seasonal change.

0.160	0.10--0.16	Evergreen Forest	Areas dominated by trees generally greater than 5 meters tall, and greater than 20% of total vegetation cover. More than 75 percent of the tree species maintain their leaves all year. Canopy is never without green foliage.
0.160	0.10--0.16	Mixed Forest	Areas dominated by trees generally greater than 5 meters tall, and greater than 20% of total vegetation cover. Neither deciduous nor evergreen species are greater than 75 percent of total tree cover.
0.100	0.07--0.16	Shrub/Scrub	Areas dominated by shrubs; less than 5 meters tall with shrub canopy typically greater than 20% of total vegetation. This class includes true shrubs, young trees in an early successional stage or trees stunted from environmental conditions.
0.035	0.025--0.05	Grassland/Herbaceous	Areas dominated by grammanoid or herbaceous vegetation, generally greater than 80% of total vegetation. These areas are not subject to intensive management such as tilling, but can be utilized for grazing.
0.030	0.025--0.05	Pasture/Hay	Areas of grasses, legumes, or grass-legume mixtures planted for livestock grazing or the production of seed or hay crops, typically on a perennial cycle. Pasture/hay vegetation accounts for greater than 20 percent of total vegetation.
0.035	0.025--0.05	Cultivated Crops	Areas used for the production of annual crops, such as corn, soybeans, vegetables, tobacco, and cotton, and also perennial woody crops such as orchards and vineyards. Crop vegetation accounts for greater than 20 percent of total vegetation. This class also includes all land being actively tilled.
0.120	0.045--0.15	Woody Wetlands	Areas Where forest or shrub land vegetation accounts for greater than 20 percent of r substrate is periodically saturated with or covered with water.
0.070	0.05--0.085	Emergent Herbaceous Wetlands	Areas where perennial herbaceous vegetation accounts for greater than 80 percent of vegetative cover and the soil or substrate is periodically saturated with or covered with water.

Appendix F: Land Use/Cover Map of 2D Flow Area Downstream of Lower Awash Dam

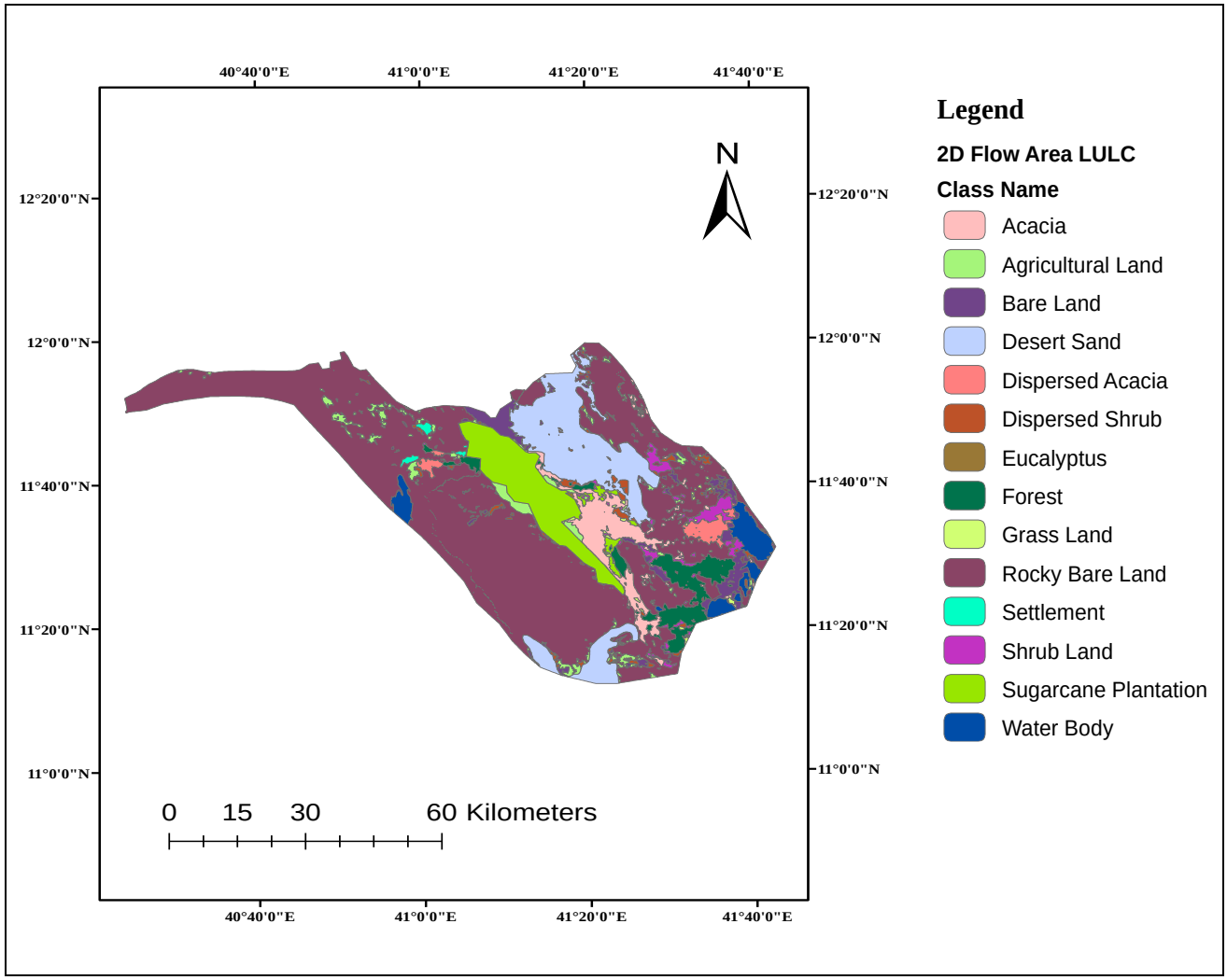

Figure F1: Land Use/Cover Map of 2D Flow Area

Appendix G: Breach Station and Elevation

Table G1: Breach Station and Elevation for Piping Failure Mode

Breach Station and Elevation for Piping Failure Mode				
Von Thun & Gillete			Froehlich (2008)	
Station(x)	Elevation(y)		Station(x)	Elevation(y)
88	771		61.9	771
112	723		95.5	723
258	723		274.5	723
282	771		308.1	771

Appendix H: Breach Outflow Discharge for Piping Failure

Date	Breach Outflow (m3/s)	Date	Breach Outflow (m3/s)	Date	Breach Outflow (m3/s)	Date	Breach Outflow (m3/s)	Date	Breach Outflow (m3/s)
01Jul2019 0000	0	03Jul2019 0000	17496	05Jul2019 0000	12060	07Jul2019 0000	9653	09Jul2019 0000	8394
01Jul2019 0100	0	03Jul2019 0100	17364	05Jul2019 0100	12009	07Jul2019 0100	9629	09Jul2019 0100	8376
01Jul2019 0200	0	03Jul2019 0200	17208	05Jul2019 0200	11956	07Jul2019 0200	9602	09Jul2019 0200	8359
01Jul2019 0300	0	03Jul2019 0300	17040	05Jul2019 0300	11903	07Jul2019 0300	9573	09Jul2019 0300	8341
01Jul2019 0400	0	03Jul2019 0400	16866	05Jul2019 0400	11851	07Jul2019 0400	9544	09Jul2019 0400	8324
01Jul2019 0500	0	03Jul2019 0500	16346	05Jul2019 0500	11799	07Jul2019 0500	9515	09Jul2019 0500	8307
01Jul2019 0600	0	03Jul2019 0600	16284	05Jul2019 0600	11749	07Jul2019 0600	9487	09Jul2019 0600	8290
01Jul2019 0700	0	03Jul2019 0700	16152	05Jul2019 0700	11699	07Jul2019 0700	9458	09Jul2019 0700	8274
01Jul2019 0800	0	03Jul2019 0800	15995	05Jul2019 0800	11649	07Jul2019 0800	9430	09Jul2019 0800	8257
01Jul2019 0900	0	03Jul2019 0900	15829	05Jul2019 0900	11598	07Jul2019 0900	9402	09Jul2019 0900	8242
01Jul2019 1000	0	03Jul2019 1000	15668	05Jul2019 1000	11545	07Jul2019 1000	9375	09Jul2019 1000	8226
01Jul2019 1100	1	03Jul2019 1100	15518	05Jul2019 1100	11493	07Jul2019 1100	9348	09Jul2019 1100	8211
01Jul2019 1200	1	03Jul2019 1200	15134	05Jul2019 1200	11441	07Jul2019 1200	9322	09Jul2019 1200	8196
01Jul2019 1300	1	03Jul2019 1300	14914	05Jul2019 1300	11417	07Jul2019 1300	9296	09Jul2019 1300	8181
01Jul2019 1400	2	03Jul2019 1400	14894	05Jul2019 1400	11419	07Jul2019 1400	9270	09Jul2019 1400	8166
01Jul2019 1500	4	03Jul2019 1500	14825	05Jul2019 1500	11414	07Jul2019 1500	9246	09Jul2019 1500	8152
01Jul2019 1600	6	03Jul2019 1600	14735	05Jul2019 1600	10899	07Jul2019 1600	9222	09Jul2019 1600	8138
01Jul2019 1700	9	03Jul2019 1700	14636	05Jul2019 1700	10899	07Jul2019 1700	9198	09Jul2019 1700	8124
01Jul2019 1800	13	03Jul2019 1800	14534	05Jul2019 1800	10896	07Jul2019 1800	9175	09Jul2019 1800	8110
01Jul2019 1900	20	03Jul2019 1900	14433	05Jul2019 1900	10895	07Jul2019 1900	9151	09Jul2019 1900	8097
01Jul2019 2000	30	03Jul2019 2000	14333	05Jul2019 2000	10891	07Jul2019 2000	9127	09Jul2019 2000	8083
01Jul2019 2100	45	03Jul2019 2100	14236	05Jul2019 2100	10867	07Jul2019 2100	9104	09Jul2019 2100	8070
01Jul2019 2200	63	03Jul2019 2200	14144	05Jul2019 2200	10833	07Jul2019 2200	9080	09Jul2019 2200	8057
01Jul2019 2300	87	03Jul2019 2300	14058	05Jul2019 2300	10795	07Jul2019 2300	9056	09Jul2019 2300	8044
02Jul2019 0000	114	04Jul2019 0000	14033	06Jul2019 0000	10755	08Jul2019 0000	9033	10Jul2019 0000	8032
02Jul2019 0100	144	04Jul2019 0100	13524	06Jul2019 0100	10713	08Jul2019 0100	9028	10Jul2019 0100	8020
02Jul2019 0200	174	04Jul2019 0200	13512	06Jul2019 0200	10671	08Jul2019 0200	9028	10Jul2019 0200	8007
02Jul2019 0300	206	04Jul2019 0300	13512	06Jul2019 0300	10629	08Jul2019 0300	9026	10Jul2019 0300	7995
02Jul2019 0400	240	04Jul2019 0400	13491	06Jul2019 0400	10586	08Jul2019 0400	9026	10Jul2019 0400	7983
02Jul2019 0500	274	04Jul2019 0500	13439	06Jul2019 0500	10545	08Jul2019 0500	8915	10Jul2019 0500	7970
02Jul2019 0600	714	04Jul2019 0600	13373	06Jul2019 0600	10504	08Jul2019 0600	8544	10Jul2019 0600	7957
02Jul2019 0700	**60072**	04Jul2019 0700	13301	06Jul2019 0700	10463	08Jul2019 0700	8537	10Jul2019 0700	7944
02Jul2019 0800	50763	04Jul2019 0800	13225	06Jul2019 0800	10423	08Jul2019 0800	8539	10Jul2019 0800	7931
02Jul2019 0900	40435	04Jul2019 0900	13147	06Jul2019 0900	10384	08Jul2019 0900	8539	10Jul2019 0900	7918
02Jul2019 1000	29786	04Jul2019 1000	13068	06Jul2019 1000	10345	08Jul2019 1000	8534	10Jul2019 1000	7907
02Jul2019 1100	35739	04Jul2019 1100	12989	06Jul2019 1100	10307	08Jul2019 1100	8537	10Jul2019 1100	7906
02Jul2019 1200	31282	04Jul2019 1200	12909	06Jul2019 1200	10270	08Jul2019 1200	8537	10Jul2019 1200	7906
02Jul2019 1300	26100	04Jul2019 1300	12830	06Jul2019 1300	10233	08Jul2019 1300	8536	10Jul2019 1300	7905
02Jul2019 1400	23047	04Jul2019 1400	12751	06Jul2019 1400	10197	08Jul2019 1400	8535	10Jul2019 1400	7906
02Jul2019 1500	21138	04Jul2019 1500	12699	06Jul2019 1500	10194	08Jul2019 1500	8534	10Jul2019 1500	7906
02Jul2019 1600	20105	04Jul2019 1600	12402	06Jul2019 1600	10192	08Jul2019 1600	8529	10Jul2019 1600	7906
02Jul2019 1700	19246	04Jul2019 1700	12187	06Jul2019 1700	9696	08Jul2019 1700	8518	10Jul2019 1700	7906
02Jul2019 1800	18919	04Jul2019 1800	12175	06Jul2019 1800	9690	08Jul2019 1800	8504	10Jul2019 1800	7906
02Jul2019 1900	18644	04Jul2019 1900	12172	06Jul2019 1900	9689	08Jul2019 1900	8488	10Jul2019 1900	7904
02Jul2019 2000	18412	04Jul2019 2000	12169	06Jul2019 2000	9690	08Jul2019 2000	8470	10Jul2019 2000	7905
02Jul2019 2100	17813	04Jul2019 2100	12170	06Jul2019 2100	9690	08Jul2019 2100	8451	10Jul2019 2100	7905
02Jul2019 2200	17757	04Jul2019 2200	12148	06Jul2019 2200	9687	08Jul2019 2200	8431	10Jul2019 2200	7907
02Jul2019 2300	17624	04Jul2019 2300	12109	06Jul2019 2300	9674	08Jul2019 2300	8413	10Jul2019 2300	7630

Date	Breach Outflow (m3/s)	Date	Breach Outflow (m3/s)	Date	Breach Outflow (m3/s)	Date	Breach Outflow (m3/s)	Date	Breach Outflow (m3/s)
11Jul2019 0000	7440	13Jul2019 0000	7214	15Jul2019 0000	7078	17Jul2019 0000	7077	19Jul2019 0000	7077
11Jul2019 0100	7440	13Jul2019 0100	7208	15Jul2019 0100	7078	17Jul2019 0100	7077	19Jul2019 0100	7077
11Jul2019 0200	7438	13Jul2019 0200	7202	15Jul2019 0200	7078	17Jul2019 0200	7077	19Jul2019 0200	7077
11Jul2019 0300	7440	13Jul2019 0300	7197	15Jul2019 0300	7078	17Jul2019 0300	7077	19Jul2019 0300	7077
11Jul2019 0400	7440	13Jul2019 0400	7190	15Jul2019 0400	7078	17Jul2019 0400	7077	19Jul2019 0400	7077
11Jul2019 0500	7439	13Jul2019 0500	7184	15Jul2019 0500	7078	17Jul2019 0500	7077	19Jul2019 0500	7077
11Jul2019 0600	7440	13Jul2019 0600	7177	15Jul2019 0600	7078	17Jul2019 0600	7077	19Jul2019 0600	7077
11Jul2019 0700	7440	13Jul2019 0700	7170	15Jul2019 0700	7078	17Jul2019 0700	7077	19Jul2019 0700	7077
11Jul2019 0800	7438	13Jul2019 0800	7162	15Jul2019 0800	7078	17Jul2019 0800	7077	19Jul2019 0800	7077
11Jul2019 0900	7439	13Jul2019 0900	7148	15Jul2019 0900	7078	17Jul2019 0900	7077	19Jul2019 0900	7077
11Jul2019 1000	7439	13Jul2019 1000	7131	15Jul2019 1000	7078	17Jul2019 1000	7077	19Jul2019 1000	7077
11Jul2019 1100	7439	13Jul2019 1100	7119	15Jul2019 1100	7078	17Jul2019 1100	7077	19Jul2019 1100	7077
11Jul2019 1200	7439	13Jul2019 1200	7110	15Jul2019 1200	7078	17Jul2019 1200	7077	19Jul2019 1200	7077
11Jul2019 1300	7438	13Jul2019 1300	7104	15Jul2019 1300	7078	17Jul2019 1300	7077	19Jul2019 1300	7077
11Jul2019 1400	7438	13Jul2019 1400	7099	15Jul2019 1400	7078	17Jul2019 1400	7077	19Jul2019 1400	7077
11Jul2019 1500	7436	13Jul2019 1500	7096	15Jul2019 1500	7078	17Jul2019 1500	7077	19Jul2019 1500	7077
11Jul2019 1600	7437	13Jul2019 1600	7093	15Jul2019 1600	7078	17Jul2019 1600	7077	19Jul2019 1600	7077
11Jul2019 1700	7437	13Jul2019 1700	7091	15Jul2019 1700	7078	17Jul2019 1700	7077	19Jul2019 1700	7077
11Jul2019 1800	7437	13Jul2019 1800	7089	15Jul2019 1800	7078	17Jul2019 1800	7077	19Jul2019 1800	7077
11Jul2019 1900	7436	13Jul2019 1900	7088	15Jul2019 1900	7078	17Jul2019 1900	7077	19Jul2019 1900	7077
11Jul2019 2000	7437	13Jul2019 2000	7086	15Jul2019 2000	7078	17Jul2019 2000	7077	19Jul2019 2000	7077
11Jul2019 2100	7437	13Jul2019 2100	7085	15Jul2019 2100	7078	17Jul2019 2100	7077	19Jul2019 2100	7077
11Jul2019 2200	7435	13Jul2019 2200	7084	15Jul2019 2200	7078	17Jul2019 2200	7077	19Jul2019 2200	7077
11Jul2019 2300	7432	13Jul2019 2300	7083	15Jul2019 2300	7078	17Jul2019 2300	7077	19Jul2019 2300	7077
12Jul2019 0000	7429	14Jul2019 0000	7083	16Jul2019 0000	7078	18Jul2019 0000	7077	20Jul2019 0000	7077
12Jul2019 0100	7406	14Jul2019 0100	7082	16Jul2019 0100	7078	18Jul2019 0100	7077		
12Jul2019 0200	7381	14Jul2019 0200	7081	16Jul2019 0200	7078	18Jul2019 0200	7077		
12Jul2019 0300	7361	14Jul2019 0300	7081	16Jul2019 0300	7078	18Jul2019 0300	7077		
12Jul2019 0400	7345	14Jul2019 0400	7080	16Jul2019 0400	7078	18Jul2019 0400	7077		
12Jul2019 0500	7332	14Jul2019 0500	7080	16Jul2019 0500	7078	18Jul2019 0500	7077		
12Jul2019 0600	7321	14Jul2019 0600	7080	16Jul2019 0600	7078	18Jul2019 0600	7077		
12Jul2019 0700	7311	14Jul2019 0700	7079	16Jul2019 0700	7078	18Jul2019 0700	7077		
12Jul2019 0800	7303	14Jul2019 0800	7079	16Jul2019 0800	7077	18Jul2019 0800	7077		
12Jul2019 0900	7295	14Jul2019 0900	7079	16Jul2019 0900	7077	18Jul2019 0900	7077		
12Jul2019 1000	7288	14Jul2019 1000	7079	16Jul2019 1000	7077	18Jul2019 1000	7077		
12Jul2019 1100	7281	14Jul2019 1100	7079	16Jul2019 1100	7077	18Jul2019 1100	7077		
12Jul2019 1200	7275	14Jul2019 1200	7078	16Jul2019 1200	7077	18Jul2019 1200	7077		
12Jul2019 1300	7269	14Jul2019 1300	7078	16Jul2019 1300	7077	18Jul2019 1300	7077		
12Jul2019 1400	7264	14Jul2019 1400	7078	16Jul2019 1400	7077	18Jul2019 1400	7077		
12Jul2019 1500	7258	14Jul2019 1500	7078	16Jul2019 1500	7077	18Jul2019 1500	7077		
12Jul2019 1600	7253	14Jul2019 1600	7078	16Jul2019 1600	7077	18Jul2019 1600	7077		
12Jul2019 1700	7248	14Jul2019 1700	7078	16Jul2019 1700	7077	18Jul2019 1700	7077		
12Jul2019 1800	7243	14Jul2019 1800	7078	16Jul2019 1800	7077	18Jul2019 1800	7077		
12Jul2019 1900	7238	14Jul2019 1900	7078	16Jul2019 1900	7077	18Jul2019 1900	7077		
12Jul2019 2000	7234	14Jul2019 2000	7078	16Jul2019 2000	7077	18Jul2019 2000	7077		
12Jul2019 2100	7229	14Jul2019 2100	7078	16Jul2019 2100	7077	18Jul2019 2100	7077		
12Jul2019 2200	7224	14Jul2019 2200	7078	16Jul2019 2200	7077	18Jul2019 2200	7077		
12Jul2019 2300	7219	14Jul2019 2300	7078	16Jul2019 2300	7077	18Jul2019 2300	7077		

Appendix I: Flood Hazard Potential Classification (FEMA, 2013)

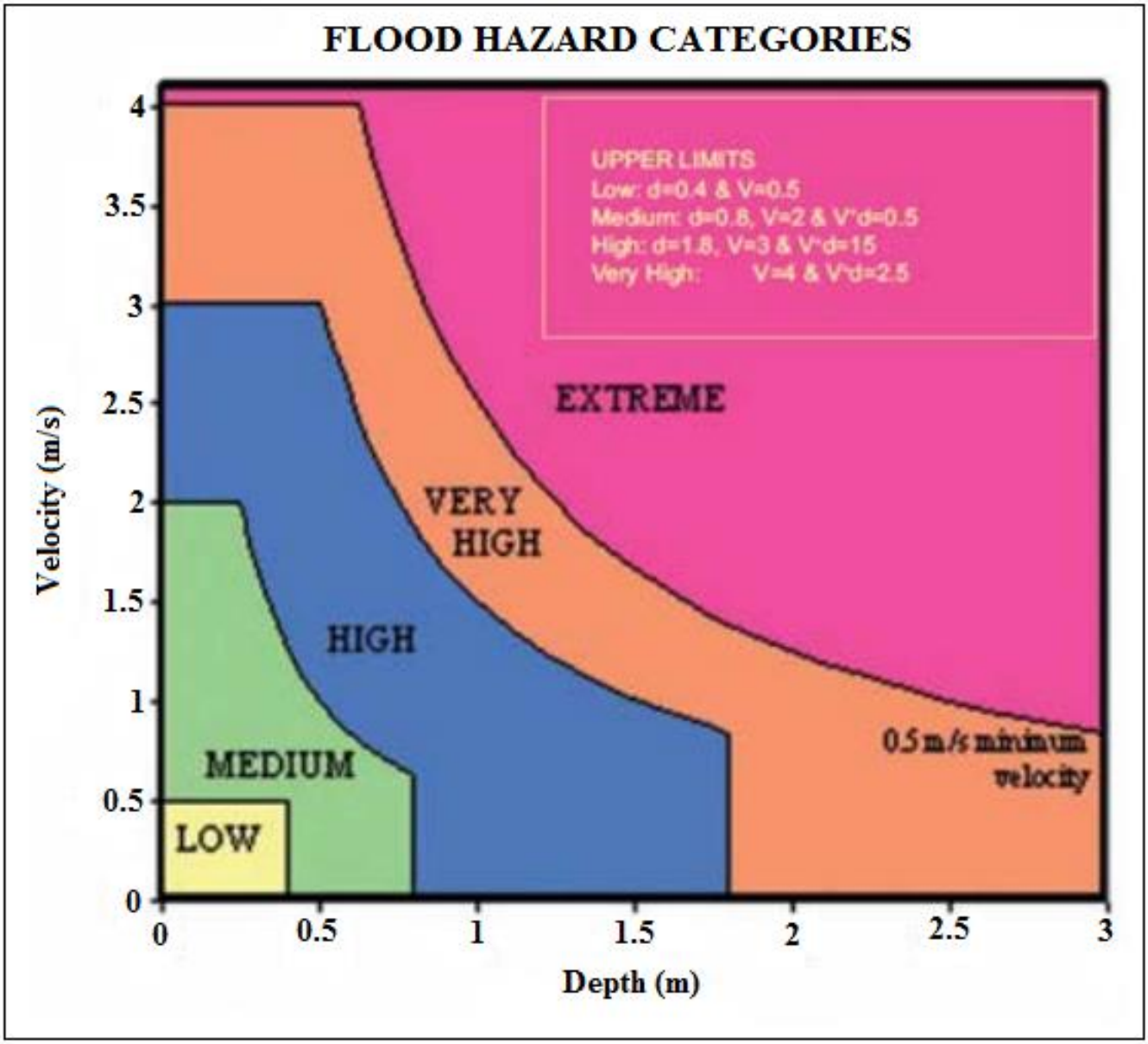

Appendix J: The Proposed Lower Awash Dam Site